Attacking Cooperative Multi-Agent Reinforcement Learning by Adversarial Minority Influence

Anonymous Authors

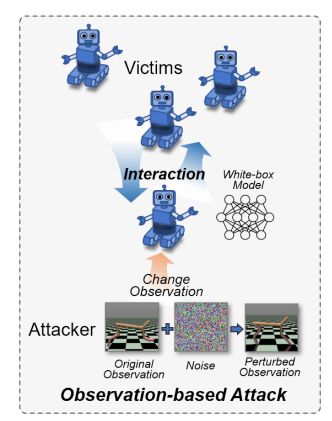
Abstract

Cooperative multi-agent reinforcement learning (c-MARL) offers a general paradigm for a group of agents to achieve a shared goal by taking individual decisions, yet is found to be vulnerable to adversarial attacks. Though harmful, adversarial attacks also play a critical role in evaluating the robustness and finding blind spots of c-MARL algorithms. However, existing attacks are not sufficiently strong and practical, which is mainly due to the ignorance of complex influence between agents and cooperative nature of victims in c-MARL.

In this paper, we propose adversarial minority influence (AMI), the first practical attack against c-MARL by introducing an adversarial agent. AMI addresses the aforementioned problems by *unilaterally* influencing other cooperative victims to a *targeted* worst-case cooperation. Technically, to maximally deviate victim policy under complex agentwise influence, our unilateral attack characterize and maximize the influence from adversary to victims. This is done by adapting a unilateral agent-wise relation metric derived from mutual information, which filters out the detrimental influence from victims to adversary. To fool victims into a jointly worst-case failure, our targeted attack influence victims to a long-term, cooperatively worst case by distracting each victim to a specific target. Such target is learned by a reinforcement learning agent in a trial-and-error process. Extensive experiments in simulation environments, including discrete control (SMAC), continuous control (MAMujoco) and real-world robot swarm control demonstrate the superiority of our AMI approach. Our codes are available in https://anonymous.4open.science/r/AMI.

1 Introduction

Cooperative multi-agent reinforcement learning (c-MARL) focuses on collaborating with a group of agents on individual policies to achieve a shared goal in an environment based on their observations. Though facing several unique challenges (e.g., combinatorial action complexity, partial observation,



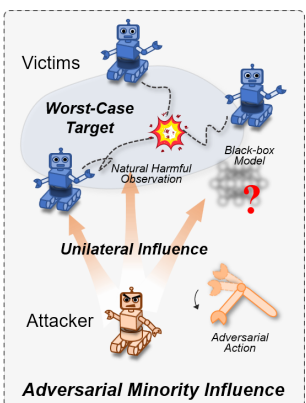


Figure 1: Comparison of different attack techniques in c-MARL. Observation-based attack requires white-box assess to agent model and adds impractical pixel-wise perturbation to agent observation. In contrast, our adversarial minority influence attack is a policy-based attack that enables one minority attacker to take legal actions that influence majority victims unilaterally towards a jointly worst target.

credit assignment, and non-stationarity [65]), current state-of-the-art c-MARL algorithms have shown promising performance in many real-world applications, including cooperative gaming [46], traffic light control [62], distributed resource allocation [70], and cooperative swarm control [20, 40, 69].

Despite the success of c-MARL, studies have revealed that c-MARL agents are vulnerable to observation-based adversarial attacks [30], where adversary adds perturbations to the observation of one agent, fooling it to take suboptimal actions. Since victim actions are intercorrelated for cooperation, other c-MARL agents would be confused and being non-robust (*c.f.* Fig. 1). Since c-MARL algorithms are typically involved in security-sensitive applications, it is important to evaluate their robustness under possible adversarial manipulations before deployment. However, the existing observation-based attack relies on white-box access to agent model and full control of agent observation, which is highly impractical. For exam-

ple, in autonomous driving, it can be prohibitively hard for attackers to assess the architectures, weights and gradients used by an vehicle, or add arbitrary pixel-wise manipulation on camera input at each timestep [18, 30, 72].

Taking a practical and black-box alternative, we perform the first *policy-based adversarial attack* (i.e., adversarial policy) [12, 15, 63] to evaluate the robustness of c-MARL. In contrast to direct observation manipulation, policy-based attacks perturb observation in a natural way: it owns an adversarial agent in c-MARL environment, which is possible in many c-MARL applications. For example, the adversary can legally join in distributed resource allocation clusters as an individual worker [6, 61, 67, 70], or control its own car in autonomous driving with multiple agents [2, 37, 49, 74]. Through interacting with the environment, the adversary learns an adversarial policy, which guides the adversary to take physically realistic actions that adversarially affect the observation of victims.

While policy-based attacks are explored in two-agent competitive games [12, 15, 63], they overlooked two important challenges in c-MARL, results in weak attack capability. Ideally, adversary should *influence* victims towards a *cooperatively* worst policy. This brings (1) the *influence* problem. In c-MARL, all agents influence each other, attacking one victim affects the policy of other victims as well. Under such complex agent-wise influence, it is hard for adversary to maximally deviate victim policies and explore the optimal attack policy. (2) The *cooperation* problem. For adversary, perturbing victim actions arbitrarily or towards locally worst case does not sufficiently indicate the failure of cooperative victims. It is challenging for adversary to explore and fool victims towards a long-term jointly worst failure case.

To address the above challenges, we propose Adversarial Minority Influence (AMI) as the first adversarial policy attack for c-MARL. As shown in Fig. 1, AMI differs from other attacks by fooling victims in a unilateral and targeted way. The name *minority influence* comes from social psychology [10], where a persistent minority (adversary) could unilaterally persuade majorities (victims) to accept his own target believe. Technically, to maximally deviate victim policies under complex agent interactions, we quantify and maximize the adversarial effect from adversary to each victim. Our unilateral influence filter adapts mutual information, a bilateral agent-wise relation metric to a unilateral relation that reflects the impact from adversary to victim. This is done by decomposing mutual information and filtering out the detrimental influence from victims to adversary. To fool victims into a jointly wort-case failure, we influence each victim to their own target, which jointly forms a worst-case long-term failure. The target is learned by targeted adversarial oracle, a reinforcement learning agent that generates worst-case target actions for each victim by co-adapting with our adversarial policy. Finally, attacker changes its policy to lead victims toward this adversarial target actions by unilateral influence. Our contributions can be summarized as:

- We design AMI, a strong and practical attack as the first adversarial policy towards c-MARL, which can better address the complex influence between agents and better handling cooperative nature of victims in c-MARL.
- We propose the unilateral influence filter and targeted adversarial oracle to maximize victim policy deviation and fool victims into worst cooperation, leading to strong attack capability.
- Extensive experiments on discrete control (SMAC environment), continuous control (MAMujoco environment), and real-world robot swarm control demonstrate the effectiveness of our AMI approach.

2 Related Work

2.1 Overview of Adversarial Attacks

First proposed in computer vision, adversarial attacks are elaborately designed perturbations that are imperceptible to humans but could fool deep neural networks (DNNs) to wrong predictions [4, 13, 53]. Given DNN F_{θ} , clean image \mathbf{x} , perturbed image \mathbf{x}_{adv} , ground truth label y, the adversarial example could be formalized as:

$$\mathbb{F}_{\theta}(x_{adv}) \neq y \quad s.t. \quad \|\mathbf{x} - \mathbf{x}_{adv}\| \leq \varepsilon,$$
 (1)

where $\|\cdot\|$ is a distance metric to constrain the distance between \mathbf{x} and \mathbf{x}_{adv} by ε . Later, it was shown that reinforcement learning (RL) is also vulnerable to adversarial attack [18, 26, 31]. Due to the sequential decision-making nature of RL, adversarial attacks in RL aim to generate a perturbation policy π^{α} that minimizes the cumulative reward $\sum_{t} \gamma' r_{t}$ of the victim, which could be written as:

$$\min_{\pi^{\alpha}} \sum_{t} \gamma^{t} r_{t}. \tag{2}$$

Note that adversarial attack is a test-time attack, in which adversary targets a fixed victim and does not involve in training process. In contrast, training-time attacks perturb victim training, such that trained victims will fail to perform well (poisoning attack) [19,41,60] or will perform adversary-specified actions with the presence of specific triggers (backdoor attack) [1,25,58,66]. Technically, training-time attacks can be achieved by modifying observation [1,25,66], trajectories [58,60] or reward [19,41]. Since our AMI is a test-time attack, our method is irrelevant to training-time attacks.

2.2 RL Attacks by Observation Perturbation

By perturbing RL observations at test time, an attacker can fool the policy network of RL agents to perform suboptimal actions, which fail RL agents to achieve their goal. *To attack single-agent RL*, early works rely on heuristics, such as

victims do not select the best action [18], or select actions with lowest value at critical timesteps [26, 31]. Later works formulate adversary and victim in an MDP framework [72]. In this way, the "optimal" perturbation on observation could be learned as an action under the current state using an RL agent [51,71]. To attack c-MARL, Lin et al. [30] propose a two-step attack. First, the attacker learns a worst-case attack policy. Then, a gradient-based attack [13,38] is used to execute that policy. However, [30] assumes attacker can modify victim observations and has white-box access to victim parameters, which can be impractical in real world. Another line of work called adversarial message targets communicative c-MARL. Adversary focus on sending messages to other victim agents, which fail victims once observing the adversarial message. The adversarial message can be added on representation [56] or learned by the adversary [3, 35, 64]. However, their method cannot be applied if victim agents do not communicate, which is assumed by various mainstream c-MARL algorithms [9, 33, 42, 68].

2.3 RL Attacks by Adversarial Policy

Different from observation-based attacks, adversarial policy requires no access to victim observation and victim parameters (black-box). Instead, it introduces an adversarial agent that uses its actions to attack victim agents, such that fooled victim agents will take counter-intuitive actions and fail to achieve their goal. In this paper, we use policy-based attack and adversarial policy interchangeably. Gleave et al. [12] first introduce adversarial policy in two-agent zero-sum games. Later works improve adversarial policy by exploiting the weakness of victim agents. Wu et al. [63] create larger deviation in victim action by perturbing the most sensitive feature in victim observation, found by a saliency-based approach. However, larger deviations in victim actions does not indicate strategically worse policy. Guo et al. [15] extend adversarial policies to general-sum games by jointly maximizing reward of adversary and minimizing rewards of victim. However, none of these works consider attack in c-MARL settings.

2.4 Training c-MARL agents

Training c-MARL agents require multiple agents learn to work cooperatively to achieve highest joint reward. Early works such as IQL [54] train each agent individually. Later methods focus on solving the credit assignment problem, the goal is to decompose the joint value function, such that each agent contributes to team success. Works in this line includes VDN [52], QMIX [42], COMA [9], QTRAN [50], QPLEX [57] and FACMAC [40]. Another line of works forces cooperation by training decentralized agents using a centralized critic, including MADDPG [33], IPPO [7] and MAPPO [68]. Other interesting works include forcing cooperation by maximizing mutual information, or "influence", be-

tween agents. This line of work includes social influence [21], EITI/EDTI [59], VM3-AC [24] and PMIC [29]. In this paper, we train our c-MARL victims with MAPPO [68] since it works well under both continuous and discrete control. After victims are trained, we fix their parameters during attack.

3 Threat Model

In this section, we provide a detailed illustration of policybased attack in c-MARL scenario.

3.1 Problem Definition

We define adversarial attack towards c-MARL agents as a form of partially observable Markov game [32], which can be defined by a set of elements $\langle \{N^{\alpha}, N^{\nu}\}, \mathcal{S}, \mathcal{O}, \{\mathcal{A}^{\alpha}, \mathcal{A}^{\nu}\}, \mathcal{T}, \{R^{\alpha}, R^{\nu}\}, \gamma \rangle$.

- N^{α} and N^{ν} are the number of adversary agents and victim agents, respectively. In the rest of the paper, we use α to denote adversary and ν to denote victims, respectively. When $N^{\alpha} = N^{\nu} = 1$, the problem reduce to two-agent adversarial policy [12, 15, 63].
- S is the global environmental state. Follow centralized training and decentralized execution (CTDE) [9, 33, 42, 68] paradigm in c-MARL, S is used in training only, and not in testing (execution).
- $O := O_1 \times ... \times O_{N^{\text{v}} + N^{\alpha}}$ is the local observation of victims and adversary. Individual observation O_i is given to the policy network of victims and adversaries as input.
- $\mathcal{A}^{\mathsf{v}} := A_{N^{\mathsf{v}}}^{\mathsf{v}} \times ... \times A_{N^{\mathsf{v}}}^{\mathsf{v}}$ and $\mathcal{A}^{\alpha} := A_{1}^{\alpha} \times ... \times A_{N^{\mathsf{v}}}^{\alpha}$ is the action taken by victims and adversaries, respectively. Victims and adversaries select actions using their own policy $\pi^{\mathsf{v}}(a^{\mathsf{v}}|o_{i}) : O \mapsto \mathcal{A}^{\mathsf{v}}$ and $\pi^{\alpha}(a^{\alpha}|o_{i}) : O \mapsto \mathcal{A}^{\alpha}$, where o_{i} is the observation of each individual agent.
- $\mathcal{T}: \mathcal{S} \times \{\mathcal{A}^{\alpha}, \mathcal{A}^{\mathbf{v}}\} \mapsto \mathcal{S}$ is the environment transition function. Given state $s \in \mathcal{S}$ and joint action $\{\mathbf{a}^{\mathbf{v}} \in \mathcal{A}^{\mathbf{v}}, \mathbf{a}^{\alpha} \in \mathcal{A}^{\alpha}\}$ at current timestep, $\mathcal{T}(s'|s, \mathbf{a}^{\alpha}, \mathbf{a}^{\mathbf{v}})$ calculates the probability of state $s' \in \mathcal{S}$ at next timestep.
- $\mathcal{R}^{\mathsf{v}}, \mathcal{R}^{\alpha}: \mathcal{S} \times \{\mathcal{A}^{\alpha}, \mathcal{A}^{\mathsf{v}}\} \times \mathcal{S} \mapsto \mathbb{R}$ denotes the reward function of victims and adversaries, after taking joint action $\{\mathbf{a}^{\mathsf{v}} \in \mathcal{A}^{\mathsf{v}}, \mathbf{a}^{\alpha} \in \mathcal{A}^{\alpha}\}$ that transitions from $s \in \mathcal{S}$ to $s' \in \mathcal{S}$. Adversaries and victims form a zero-sum game if $\mathcal{R}^{\mathsf{v}} = -\mathcal{R}^{\alpha}$, and form a general-sum game otherwise.
- γ is the discount factor over time.

The goal of attacker is to learn policy $\pi_{\theta}^{\alpha}(a^{\alpha}|o_i)$ parameterized by θ to maximize the discounted accumulated reward of attacker, $J(\theta) = \mathbb{E}_{s,\mathbf{a}}[\sum_t \gamma' r_t^{\alpha}]$, where $r_t^{\alpha} \in R^{\alpha}$. The parameters of victim policies are fixed during attack, which is common for deploying reinforcement learning agents stably [17]. In this paper, we assume there is only one attacker (*i.e.*, $N^{\alpha} = 1$)

for simplicity. To realize this adversarial attack, adversary can influence victim policies by taking adversarial actions $a^{\alpha} \in \mathcal{A}^{\alpha}$ learned by policy π^{α} at time t, which change the observation O through environment transition and misleads victims policies π^{ν} to yield inferior actions at time t+1.

3.2 Attacking Pathways and Applications

We propose two possible ways for attackers to launch our AMI attack. The first and most practical way is through legally participating in a multi-agent distributed system [23, 44] and launch adversarial policy as an individual agent. In applications such as autonomous driving [2, 37, 49, 74], distributed source allocation [6,61,67,70] and transmit power control [22, 73], adversary can legally join in the environment and take its own actions. Second, adversary can also attack by hijacking an agent directly [11,34,43], then use this controlled agent to perform adversarial policy. For example, adversary can hack in one unmanned aerial vehicles (UAV) in UAV swarms, and take adversarial actions to fool victims in applications like surveillance [69] and delivery [28].

Apart from malicious use, our AMI attack also serves as a strong testing algorithm [14] to evaluate the robustness of c-MARL algorithms under a practical threat model. Since c-MARL algorithms are shown to be non-robust against our AMI attack, it would be beneficial to test the worst-case performance of c-MARL agents using our AMI algorithm, which aids researchers to design robust algorithms and help policy makers to manage algorithmic risk before deployment.

3.3 Adversary's Constraint and Capability

We detail the constraint and capability of policy-based adversary in c-MARL attack. During attack, the adversary can fully control the adversary agent and take any physically realistic actions possible in its environment. The adversary learns an adversarial policy by taking local observation as input and take actions to influence victims at each timestep. During training, the adversarial policy is learned by interacting with victims in a trial-and-error process, typically in a simulation environment. To minimize global team reward, following assumptions commonly accepted by adversarial attacks in c-MARL [3, 30, 35, 56], adversary assess to the state and adversary rewards in training only.

As a black-box adversarial attack towards c-MARL agents, our attacker is less constrained and more practical comparing with previous white-box observation-based attack [30]. Specifically, our attacker cannot manipulate agent observation directly, but can only influence the victim observation by interacting with the environment through its own actions. Our attacker also cannot assess to models (*e.g.*, architectures, weights, gradients) of other agents. Additionally, different from previous general-sum adversarial policy used by *Guo et al.*, we assume the adversary cannot acquire victim reward

due to black-box constraint. The adversary cannot choose which agent to take over and cannot switch from controlling its current agent to another agent in different timesteps.

Additionally, for attacks in real world, our adversary do not learn in true physical world environment, but follow a Sim2Real paradigm [17] widely used in reinforcement learning community, such that adversary train its adversarial policy in simulation environment first, then freeze the parameter of its policy and deploy the attack to real world robots.

4 Adversarial Minority Influence Approach

As we have mentioned above, adversarial policy towards c-MARL face two challenges, i.e., the influence challenge requires the adversary to maximize victim policy deviations under complex agent-wise interaction; the cooperation challenge that requires the adversary to fool agents towards a jointly worst failure. In this paper, we deal with these challenges by our adversarial minority influence (AMI) framework. As illustrated in Fig. 2, AMI achieves strong attack capability by unilaterally influencing victims towards a targeted worst-case scenario. To maximize policy deviation of victims, we propose unilateral influence filter to characterize adversarial impact from adversary to victims by decomposing the bilateral mutual information metric and filtering out the detrimental influence from victims to adversary. To influence victims towards jointly worst actions, targeted adversarial oracle is a reinforcement learning agent that co-adapts with adversary and outputs cooperatively worst-case target actions for each victim at each timestep.

4.1 Unilateral Influence Filter

In c-MARL attack, since the policy of all agents are intercorrelated, attacking one victim will affect the policy of other victims as well. Under such complex relationship, maximally deviating victim policies requires the adversary to first characterize the influence of its action on each victim, then maximize such influence. Therefore, to characterize the unilateral influence from adversary to victim, inspired by minority influence theory in social psychology [5, 10], we adapt bilateral agentwise influence metric (*i.e.*, mutual information) to c-MARL attack scenario. Since the policy of adversary and victims are mutually dependent, our adversarial influence filters out the detrimental influence from victim to adversary.

We start from analyzing mutual information, a widely used bilateral influence metric in c-MARL literature [8,21,29,59] that depicts the relation between agents. Taking social influence [21] as an example, the mutual information between adversary action a_t^{α} and influenced victim action $a_{t+1,i}^{\nu}$ can be written as $I(a_t^{\alpha}; a_{t+1,i}^{\nu}|s_t, \mathbf{a}_t^{\nu})$, where a_t^{α} refers to action taken by adversary α at time t, and $a_{t+1,i}^{\nu}$ refers to action taken by the i^{th} victim ν at time t+1. In practice, since victim

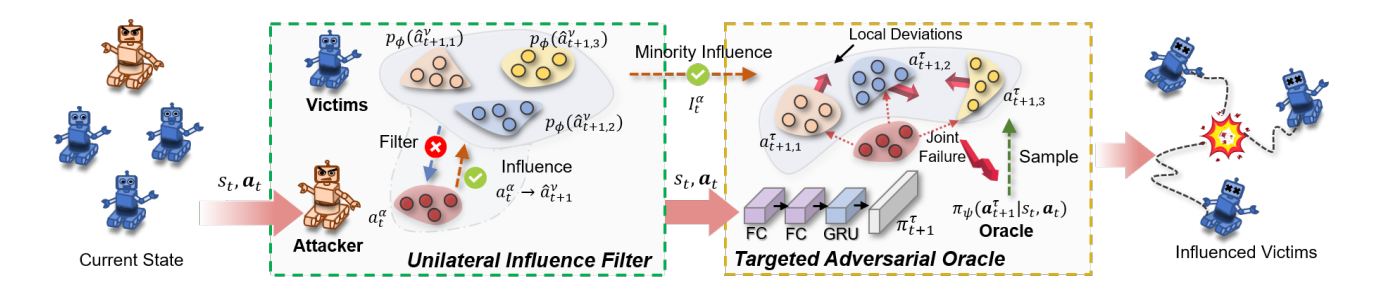


Figure 2: Framework of AMI. Unilateral influence filter decompose mutual information into minority influence and majority influence terms, while keeping latter for asymmetric influence. Targeted adversarial oracle is an RL agent that generates a worst-case target for each victim. Attacking victims towards this target results in jointly worst cooperation.

observation and parameters are unknown, the action probability of $a_{t+1,i}^{\mathsf{V}}$ is approximated by a DNN parameterized by ϕ , and trained via standard supervised learning objective, *i.e.*, $\max_{\phi} \sum_{i=1}^{N^{\mathsf{V}}} \sum_{t=0}^{T-1} \log p_{\phi}(\hat{a}_{t+1,i}^{\mathsf{V}}|s_t,\mathbf{a}_t)$, where T is the total timestep of an episode. In the rest of our paper, we use \hat{a} to denote the action is predicted, instead of ground truth.

Albeit mutual information can characterize agent-wise influence in c-MARL, attacks towards c-MARL is different since victims parameters are fixed, making victim actions harder to change than adversary. To illustrate the impact of fixed victim policy, we decompose the mutual information between adversary action a_t^{α} and a victim agent $a_{t+1,i}^{\gamma}$ as:

$$I(a_{t}^{\alpha}; \hat{a}_{t+1,i}^{\nu}|s_{t}, \mathbf{a}_{t}^{\nu}) = \underbrace{-H(\hat{a}_{t+1,i}^{\nu}|s_{t}, a_{t}^{\alpha}, \mathbf{a}_{t}^{\nu})}_{\text{majority}} + \underbrace{H(\hat{a}_{t+1,i}^{\nu}|s_{t}, \mathbf{a}_{t}^{\nu})}_{\text{minority}}.$$
(3)

In c-MARL attack, we call the first term *majority influence*, *i.e.*, how minority (attacker) changes its policy to overfit the policy of majorities (victims). To maximize mutual information, $H(\hat{a}_{t+1,i}^{v}|s_{t},a_{t}^{\alpha},\mathbf{a}_{t}^{\nu})$ should be *minimized*, such that knowing a_{t}^{α} reduces the uncertainty of victim policy. In policy-based attacks in c-MARL, majority influence term in mutual information results in attackers conforming to victim policies, leading to high mutual information but weak attack capability. To explain this, recall the parameters of victims are fixed while adversary policy is learned, we assume it is much easier to change the policy of the adversary than to change the victim policy. Thus, to minimize majority influence, the best way for an attacker is to change its action a_{t}^{α} to make it more predictive of $a_{t+1,i}^{\nu}$, while not actually changing $a_{t+1,i}^{\nu}$. Meanwhile, the second term $H(\hat{a}_{t+1,i}^{\nu}|s_{t},a_{t}^{\nu})$ can be viewed

Meanwhile, the second term $H(\hat{a}_{t+1,i}^{\mathsf{V}}|s_t,\mathbf{a}_t^{\mathsf{V}})$ can be viewed as a kind of *minority influence* free of victim impact, showing the effect of the adversary on victims only. In this term, the entropy of victim policy without conditioning on a_t^{α} is taken into account, forming an *unilateral* metric. Since the impact of adversary action a_t^{α} is marginalized out, the adversary cannot change its action to cater to victims. *To better understand majority and minority influence, we add a toy example in*

supplementary materials where we carefully illustrate the two type of influence via experiment.

Based on the above discussions, we analyze and generalize minority influence in mutual information for better attack capability. Specifically, maximizing minority influence requires current adversary policy to have large uncertainty in victim policy, which can also be written as (*see derivation in supplementary material*):

$$H(\hat{a}_{t+1,i}^{\mathsf{V}}|s_{t},\mathbf{a}_{t}^{\mathsf{V}}) = -D_{KL}\left(p_{\phi}(\hat{a}_{t+1,i}^{\mathsf{V}}|s_{t},\mathbf{a}_{t}^{\mathsf{V}})|| \mathcal{U}\right) + c$$

$$= -D_{KL}\left(\mathbb{E}_{\tilde{a}_{t}^{\alpha} \sim \pi^{\alpha}}\left[p_{\phi}(\hat{a}_{t+1,i}^{\mathsf{V}}|s_{t},\tilde{a}_{t}^{\alpha},\mathbf{a}_{t}^{\mathsf{V}})\right]|| \mathcal{U}\right) + c, \tag{4}$$

where \mathcal{U} is a uniform distribution for victim actions which applies for both discrete and random action spaces, D_{KL} is Kullback-Leibler divergence, c is a constant, \tilde{a}_t^{α} is the counterfactual action sampled from adversarial policy π_t^{α} .

Eqn. 4 points out the second term is equal to minimizing KL divergence between victim policy and uniform distribution. However, we can freely generalize \mathcal{U} to any desired target distribution \mathcal{D} and generalize D_{KL} to any distance metric $d(\cdot,\cdot)$. Thus, unilateral influence could be written as:

$$I = d\left(\mathbb{E}_{\tilde{a}_{t}^{\alpha} \sim \pi_{t}^{\alpha}} \left[p_{\phi}(\hat{a}_{t+1,i}^{\mathsf{v}} | s_{t}, \tilde{a}_{t}^{\alpha}, \mathbf{a}_{t}^{\mathsf{v}}) \right], \ \mathcal{D}) \right). \tag{5}$$

In this way, affecting victims unilaterally is equal to minimizing the distance between the expectation of victim policy under adversary policy and a target distribution.

4.2 Targeted Adversarial Oracle

After describing how to maximize victim policy deviations by unilateral influence, we still need to make sure victims are influenced towards an optimal target. Intuitively, deviating victim policy arbitrarily or towards a locally worse case does not indicate a globally worst-case failure for c-MARL. To maximize attack capability, we need to learn globally worst target actions for victims, then guide each victim to its target \mathcal{D} (Eqn. 5) via our proposed unilateral influence method. Therefore, we propose a reinforcement learning agent that learns such jointly worst target actions by co-adapting its policy with attacker in a trial-and-error process.

To achieve the targeted attack goal, we propose $\mathit{Targeted}$ $\mathit{Adversarial Oracle}$ (TAO) , a reinforcement learning agent π_{ψ} parameterized by ψ , which advice attacker to unilaterally influence each victims towards a targeted local policy. With all victims influenced in this way, they form a jointly worst case for cooperative agents. We use τ to denote the action and policy used by TAO. As an RL agent, TAO adapts to the current perturbation budget of the adversary by trial-and-error process: if the adversary could strongly affect victim policies, TAO could generate the target more radically, ordering victims to take more dangerous actions, achieving higher attack capability; if the adversary can hardly influence victims, TAO then seeks to make small but effective perturbations to victims, which is realistic under current perturbation budget.

Similar to the attacker, the goal of TAO is to maximize the goal of the adversary. Thus, we train the policy of TAO to maximize the cumulated adversarial reward r^{α} using proximal policy optimization (PPO) [48]:

$$\max_{\boldsymbol{\Psi}} \mathbb{E}_{\boldsymbol{\pi}_{\boldsymbol{\Psi}}^{\tau}} \left[\min \left(\operatorname{clip} \left(\boldsymbol{\rho}_{t}, 1 - \boldsymbol{\varepsilon}, 1 + \boldsymbol{\varepsilon} \right) \boldsymbol{A}_{t}^{\tau}, \boldsymbol{\rho}_{t} \boldsymbol{A}_{t}^{\tau} \right) \right],$$
where
$$\boldsymbol{\rho}_{t} = \frac{1}{N^{V}} \sum_{i=1}^{N^{V}} \frac{\boldsymbol{\pi}_{\boldsymbol{\Psi}}^{\tau} (\boldsymbol{a}_{t+1,i}^{\tau} | \boldsymbol{s}_{t}, \mathbf{a}_{t}^{V}, \boldsymbol{a}_{t}^{\alpha})}{\boldsymbol{\pi}_{\boldsymbol{\Psi}_{t}^{\tau}, t}^{\tau} (\boldsymbol{a}_{t+1,i}^{\tau} | \boldsymbol{s}_{t}, \mathbf{a}_{t}^{V}, \boldsymbol{a}_{t}^{\alpha})}, \tag{6}$$

where $\pi_{\psi_{old}}^{\tau}$ and π_{ψ}^{τ} denotes the old and new policy for TAO. A_t^{τ} is the advantage function calculated by generalized advantage estimation (GAE) [47]. $clip(\rho_t, 1-\epsilon, 1+\epsilon)$ trims input ρ_t at threshold $1-\epsilon$ and $1+\epsilon$.

Now, the policy $\pi^{\tau}_{\psi,i}(\cdot|s_t,\mathbf{a}_t)$ learned by TAO serves as the desired target distribution \mathcal{D} in Eqn. 5 for victim i at time t. In practice, since PPO is an on-policy algorithm, real actions must be taken at each timestep. Thus, \mathcal{D} was given by sampling a target action $a_{t+1,i}^{\tau}$ from $\pi^{\tau}_{\psi,i}$ instead.

4.3 Overall Training

Overall, the influence metric I_t^{α} used by AMI at time t combines the optimal target action $a_{t+1,i}^{\tau}$ generated by TAO as the target distribution \mathcal{D} in unilateral influence in Eqn. 5:

$$I_{t}^{\alpha} = \sum_{i=1}^{N^{\mathsf{V}}} \left[d\left(\mathbb{E}_{\tilde{a}_{t}^{\alpha} \sim \pi_{t}^{\alpha}} \left[p_{\phi}(\hat{a}_{t+1,i}^{\mathsf{V}} | s_{t}, \tilde{a}_{t}^{\alpha}, \mathbf{a}_{t}^{\mathsf{V}}) \right], \right.$$

$$\left. a_{t+1,i}^{\tau} \sim \pi_{\Psi}^{\tau}(\cdot | s_{t}, a_{t}^{\alpha}, \mathbf{a}_{t}^{\mathsf{V}}) \right) \right],$$

$$(7)$$

where $d(\cdot,\cdot)$ is the distance function for AMI. In discrete control, we calculate it as $d(p(\hat{a}_i^{\mathrm{v}}|s,\mathbf{a}),a_i^{\mathrm{v}}) = -||p(\hat{a}_i^{\mathrm{v}}|s,\mathbf{a}) - \mathbf{1}_{\mathcal{A}}(a_i^{\mathrm{v}})||_1$, where we use $p(\hat{a}_i^{\mathrm{v}}|s,\mathbf{a})$ as a shorthand for $\mathbb{E}_{a_i^{\mathrm{v}} \sim \pi_i^{\mathrm{v}}} \left[p(\hat{a}_{t+1,i}^{\mathrm{v}}|s_t,\tilde{a}_t^{\mathrm{v}},\mathbf{a}_t^{\mathrm{v}}) \right]$ and a_i^{v} as a shorthand for $a_{t+1,i}^{\mathrm{v}}$. $\mathbf{1}_{\mathcal{A}}(a_i^{\mathrm{v}}) = [a_i^{\mathrm{v}} \in \mathcal{A}_i^{\mathrm{v}}]$ is the indicator function with action space $\mathcal{A}_i^{\mathrm{v}}$. A negative sign was added to minimize the distance between one-hot target action $\mathbf{1}_{\mathcal{A}}(a_i^{\mathrm{v}})$ and victim action probability. In continuous control, the distance function was calculated as $d(p(\hat{a}_i^{\mathrm{v}}|s,\mathbf{a}),a_i^{\mathrm{v}}) = p(a_i^{\mathrm{v}}|s,\mathbf{a})$, such that target action $a_{t+1,i}^{\mathrm{v}}$

Algorithm 1 Adversarial Minority Influence Algorithm.

Input: Policy network of victim agents π^{V} , policy network of adversary agent π_{θ} , value function network of adversary agent V^{α} , network of opponent modelling p_{ϕ} , policy network of targeted adversarial oracle (TAO) π_{ψ} , value function network V^{τ} of TAO.

Output: Trained policy network of adversary agent π_{θ} .

- 1: **for** k = 0, 1, 2, ... K**do**
- 2: Perform rollout using current adversarial policy network π_{θ} and TAO agent π_{ψ}^{τ} . Collect a set of trajetories $\mathcal{D}_k = \tau_i$, where $i = 1, 2, ..., |\mathcal{D}_k|$.
- 3: Update opponent modelling model p_{ϕ} .
- 4: Calculate advantage function of TAO A_t^{τ} by GAE, using value function V^{α} and adversary reward r^{α} ; Update value function network V^{τ} of TAO.
- 5: Update the policy network π_{Ψ} of TAO using Eqn. 6;
- 6: Calculate reward r_t^{AMI} for adversary by Eqn. 8.
- 7: Calculate advantage function A_t^{α} by GAE, using value function V^{α} and reward r^{AMI} ; Update value function network V^{α} of adversary.
- 8: Update policy network π_{θ} of adversary by Eqn. 9.
- 9: end for

have high probability in estimated victim action probability distribution. We empirically find our method is insensitive to the choice of distance functions.

Finally, I_t^{α} was used as an auxiliary reward optimized by the policy of adversarial agent $\pi_{\theta}(a_t^{\alpha}|o_t^{\alpha})$ parameterized by θ . The reward r_t^{AMI} for adversarial agent π_{θ} to optimize is:

$$r_t^{AMI} = r_t^{\alpha} + \lambda \cdot I_t^{\alpha}, \tag{8}$$

where λ is a hyperparameter to tradeoff the adversary reward r_t^{α} and maximizing influence I_t^{α} towards victim agents. Again, we calculate the advantage function A_t^{α} using r_t^{AMI} by GAE [47] and train the adversary policy π_{θ} by PPO [48]:

$$\begin{aligned} & \max_{\theta} \mathbb{E}_{\pi_{\theta}^{\alpha}} \left[\min \left(\text{clip} \left(\rho_{t}, 1 - \varepsilon, 1 + \varepsilon \right) A_{t}^{\alpha}, \rho_{t} A_{t}^{\alpha} \right) \right], \\ & \text{where } & \rho_{t} = \frac{\pi_{\theta}^{\alpha} \left(a_{t}^{\alpha} | o_{t}^{\alpha} \right)}{\pi_{\theta_{old}}^{\alpha} \left(a_{t}^{\alpha} | o_{t}^{\alpha} \right)}. \end{aligned} \tag{9}$$

The overall training process is described in Alg. 1. Specifically, we first rollout K trajectories, get s_t and \mathbf{a}_t using current policy of attacker and victims. Then, we train opponent modelling module $p_{\phi}(\hat{a}_{t+1,i}^{\mathsf{v}}|s_t,\mathbf{a}_t)$ and update actor $\pi_{\psi}(\cdot|s_t,\mathbf{a}_t)$ and critic A_t^{τ} of targeted adversarial oracle. Finally, we calculate reward r_t^{AMI} using Eqn. 8 and update actor $\pi_{\theta}^{\alpha}(\cdot|o_t^{\alpha})$ and critic A_t^{α} of attacker.

5 Experiments

In this section, we conduct extensive experiments in simulation and real world environments to evaluate the attack capability of our AMI approach.

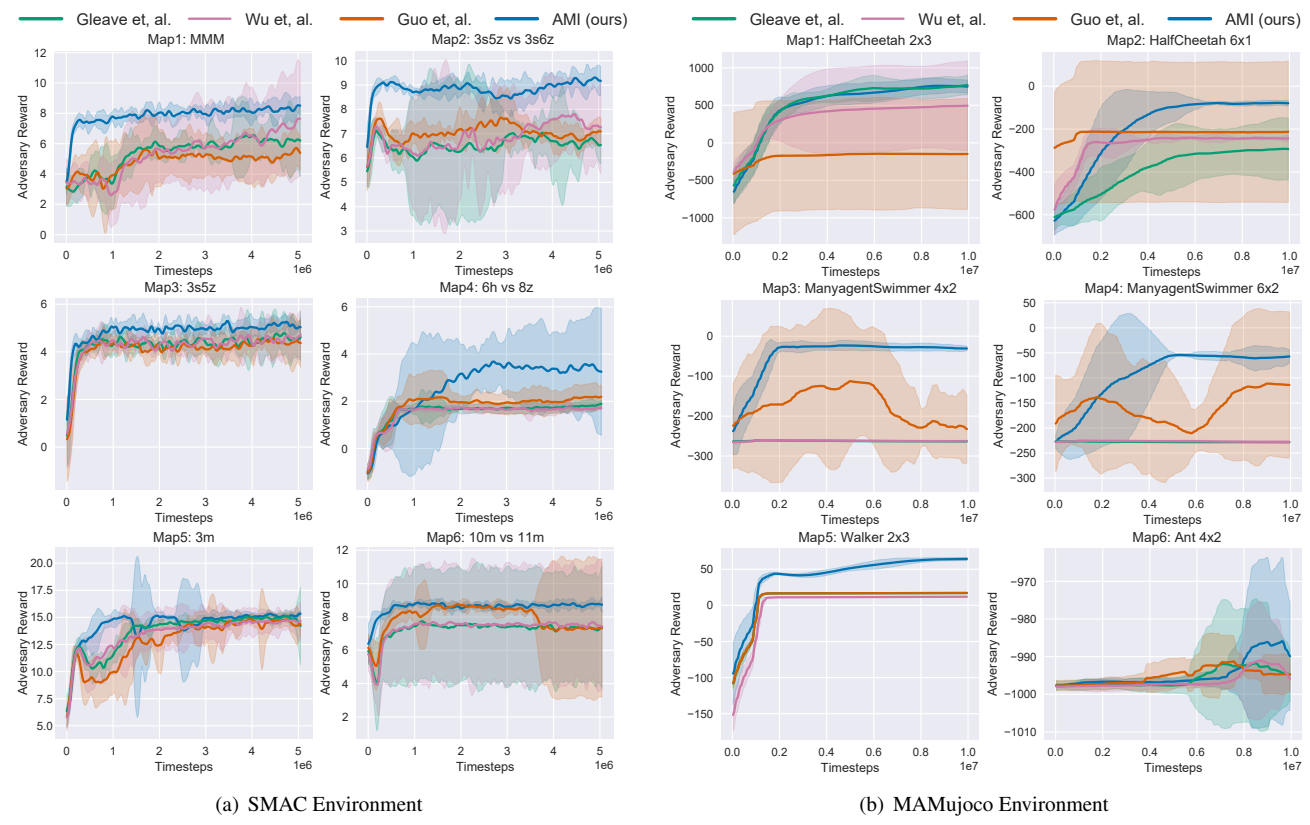


Figure 3: Learning curves for AMI and baseline attack methods in (a) six SMAC and (b) six MAMujoco environments. The solid curves correspond to the mean, and the shaped region represents the 95% confidence interval over 5 random seeds.

5.1 Experimental Setup

5.1.1 Environments and implementation details

We evaluate AMI in 3 environments: (1) StarCraft Multi-Agent Challenge (SMAC) [46] for discrete control (6 tasks), the task is to control one group of agents in StarCraft game to defeat another group of enemies; (2) Multi-Agent Mujoco (MAMujoco) [40] for continuous control (6 tasks), the task is to control joints in a robot to maximize its speed in a certain direction. (3) Real-world multi-robot rendezvous environment, where robot swarms learn to gather together. All victim policies were trained by MAPPO [68]. During attack, unless specifically stated, we select the 1st agent as adversary. *See more implementation details in supplementary materials*.

5.1.2 Compared methods and evaluation metrics

We compare AMI with current state-of-the-art adversarial policy methods including *Gleave et al.* [12], *Wu et al.* [63] and *Guo et al.* [15]. Those methods were originally proposed to attack single-agent RL, while we adapt these methods to attack c-MARL by replacing the single RL victim to multiple RL victims. To ensure fair comparison, AMI and all baselines use the same codebase, network structure, and hyperparameters. For hyperparameters specific to their method, we tune

their value to achieve the best performance.

The objective of adversary is to maximize adversary reward r^{α} , which is adapted from victim reward by adding the loss of allies, as a complement to loss of enemies (SMAC) or removing redundant auxiliary terms (MAMujoco, rendezvous). We defer detailed illustration of adversary reward in supplementary materials. In this way, similar to Guo et al., the adversary and victims form a general-sum game, while we do not require assess to victim reward. We find using our adversary reward improves overall attack capability in discussion. Consequently, we train AMI and all baselines using our adversary reward r^{α} , and use the same reward as our evaluation metric (higher means stronger attack capability). All experiments were evaluated under 5 random seeds and results were shown with a 95% confidence interval. Due to the space limit, we defer detailed baseline implementations and hyperparameters to supplementary material.

5.2 AMI Attack in Simulation Environment

In this section, we empirically evaluate if AMI is effective in simulation environments. We show our AMI is more effective comparing with baselines on six discrete control tasks (SMAC) and six continuous control tasks (MAMujoco). In all environments, we assume attacker controls the 1st agent for

simplicity. From results shown in Fig. 3, we can draw several conclusions as follows:

- (1) By unilaterally influencing victims towards a jointly worst target, AMI achieves superior results on 10 over 12 environments in both continuous and discrete control, demonstrating the effectiveness of our method.
- (2) Our experiment result points out that dimensionality controlled by adversary is not the only factor that accounts for victim vulnerability in c-MARL, which complements the claim made by *Gleave et al.* For example, under the same dimensionality, AMI achieves superior attack capability in *Swimmer 4x2*, while all attacks are ineffective in *Ant 4x2*. We hypothesize that some tasks might be intrinsically robust, possibly because of robust environment dynamics (*i.e.*, environment providing similar observation under different adversary actions), weak capability of attacker (*i.e.*, attacker controlling an insignificant agent), or weak cooperation between attacker and victims (*i.e.*, agents do not cooperate and do not condition its policy on action taken by adversary).
- (3) In environments such as 3m, all baselines converge to the same point with low variance. We hypothesize that some environments have simple dynamics and are easy to attack, such that all attacks can easily converge to optimal policy.
- (4) The method of *Guo et al.* exhibits high variance in several MAMujoco environments. We find the variance is related to the general sum setting (using victim reward) and their method (training the adversary using two critics). We pose detailed discussions in supplementary materials.

Apart from fixing adversary as the 1st agent. We also experiment the attack capability of AMI when adversary controls different agent IDs, equipping adversary with different initialization and functionalities. Results of adversary attacking through all possible agents in 3s5z vs 3s6z environment show the superiority of AMI is consistent in different adversary IDs. See detailed results in supplementary materials.

5.3 AMI Attack in Real World

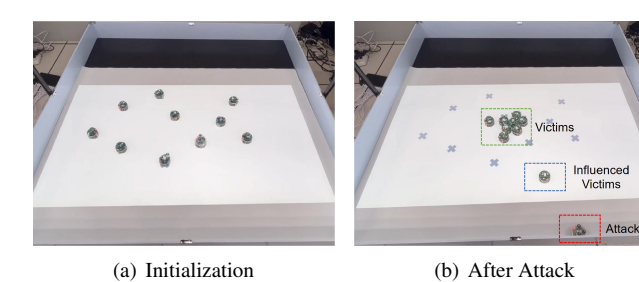


Figure 4: Illustration of our real-world multi-robot rendezvous environment. *See videos in our anonymous github.*

The real-world attack capability of adversarial policy motivates us to evaluate AMI in real-world multi-robot collaboration environments. To the best of our knowledge, this is the first demonstration of adversarial policy in the real

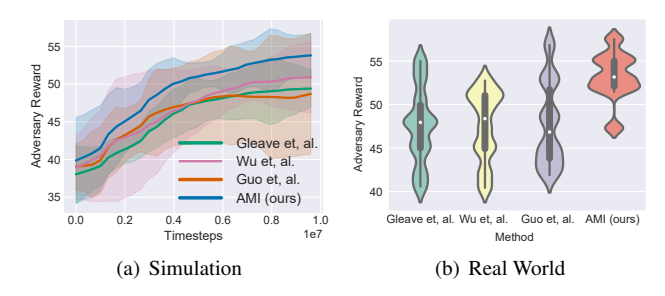


Figure 5: Comparisons of AMI against baselines in simulation and real-world experiments.

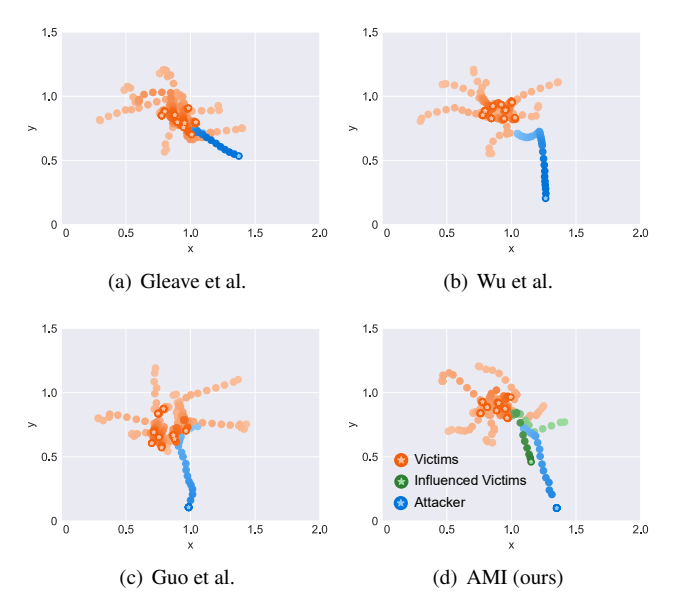


Figure 6: Comparison of the trajectories of AMI and other baselines. AMI is the only method that could fool a victim away from the gathered victims (green dots). Lighter points indicate early timesteps and darker points indicate latter timesteps. Points with a star denote the final position.

world. Specifically, we craft an environment with 10 e-puck2 robots [36] in an indoor arena, as shown in Fig. 5. The task is *rendezvous*, where robots are randomly dispersed in an arena and aim at gathering together. To mitigate the impact of initialization, our experiment uses a within-subject design, such that for all compared methods, all e-puck2 robots are initialized at the same position in the same run.

We train these robots under Sim2Real paradigm [17] widely used in RL community, such that agents first learn their policy in simulation environment, then deployed to real world with parameter fixed. To evaluate attack performance, we report results in simulation and real-world scenario in Fig. 6, with each method tested 10 times in the real world, leading to several conclusions as follows:

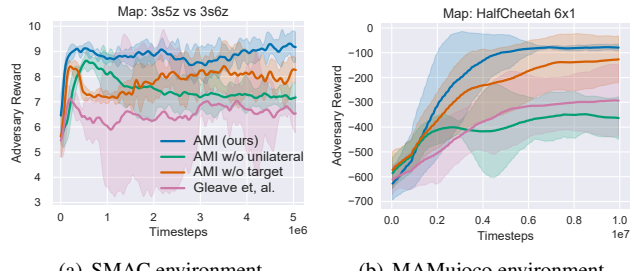
(1) Again, AMI gets better performance comparing with all baselines in both simulation and real-world environments. The improvement of AMI in the real world is significant (p < .05) than all baselines under a paired samples t test, and 5.43 higher on average comparing with the best-performing baseline in real world.

(2) Agent trajectories in Fig. 6 further show the superiority of AMI, where lighter point indicates early timesteps and darker point indicates latter timesteps. We find AMI can occasionally lure a victim to get away from gathered victims, causing green victim to first gather with majority orange victims, then fooled to move towards the adversary which maximizes adversary reward. We highlight that AMI is the only method to achieve this, with final state photoed in Fig. 4(b). See videos in our anonymous github repository.

5.4 Ablations

In this section, we verify the effectiveness of each component in our model. We conduct all experiments on 3s5z vs 3s6z for SMAC and HalfCheetah 6x1 for MAMujoco.

5.4.1 Ablations on unilateral and targeted properties



(a) SMAC environment (b) MAMujoco environment

Figure 7: Ablation of unilateral and targeted properties of AMI. Both properties improve attack performance.

First, we ablate the unilateral and targeted property of AMI. For AMI without unilateral attack, we add the majority influence term in Eqn. 3 to Eqn. 7 to make the influence bilateral. For AMI without targeted attack, we use Eqn. 4 as influence metric. We also add the result of *Gleave et al.* (*i.e.*, without unilateral and targeted attack) for comparison. As shown in Fig. 7, AMI cannot succeed without either improvement. Besides, we find AMI without unilateral property even exhibits inferior performance comparing with *Gleave et al.* in *HalfCheetah 6x1*, showing adding majority influence to our attack largely decreases attack capability, such that attacker changes its action to overfit victim policies.

5.4.2 Ablations on distance metric

Next, we study the result of AMI using different distance metrics. We list alternate distance metrics for discrete and continuous environments in Tab. 1, where $\hat{\mu}_i^{\nu}(s, \mathbf{a})$ is the mean predicted by opponent modelling for continuous control, assuming actions follow a Gaussian distribution. The result is

Table 1: Distance metrics for discrete and continuous environment. AMI is calculated by these distance metrics and maximized by attacker under the best hyperparameter λ .

Name	Equation	Environment
ℓ_1	$- p(\hat{a}_i^{v} s,\mathbf{a})-1_{\mathcal{A}}(a_i^{\tau}) _1$	Discrete
ℓ_2	$- p(\hat{a}_i^{V} s,\mathbf{a})-1_{\mathcal{A}}(a_i^{T}) _2$	Discrete
ℓ_{∞}	$- p(\hat{a}_i^{v} s,\mathbf{a})-1_{\mathcal{A}}(a_i^{t}) _{\infty}$	Discrete
CE	$\log(p(a_i^{\tau} s,\mathbf{a}))$	Discrete
Prob	$p(a_i^{\tau} s,\mathbf{a})$	Discrete
ℓ_1	$- \hat{\mu}_i^{v}(s,\mathbf{a})-a_i^{t} _1$	Continuous
CE	$\log(p(a_i^{\tau} s,\mathbf{a}))$	Continuous
Prob	$p(a_i^{\tau} s,\mathbf{a})$	Continuous

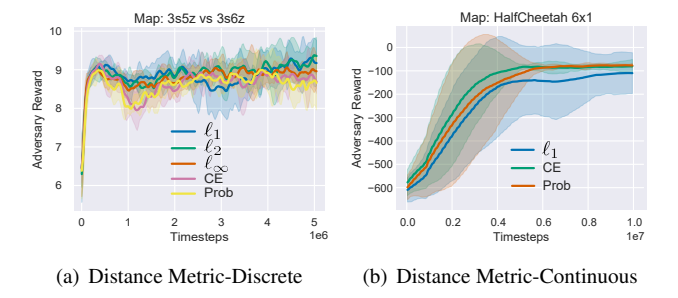


Figure 8: Ablation on distance metric. The performance of AMI is stable under different distance metrics.

illustrated in Fig. 8, indicating attack capability of AMI is insensitive under different distance metrics for both continuous and discrete control, while the metric we use (ℓ_1 for discrete control and Prob for continuous control) yields the best result.

5.4.3 Ablations on hyperparameter

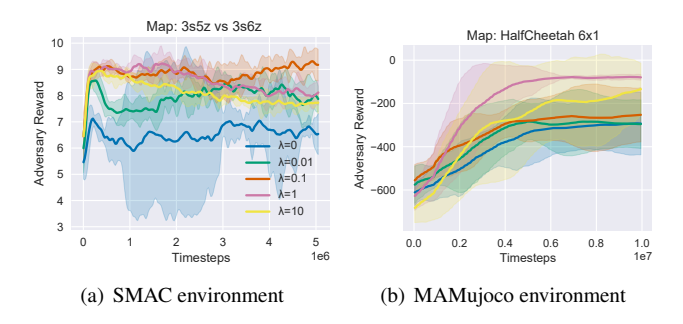


Figure 9: Ablation on hyperparameter λ . $\lambda = 0$ reduce to the method of *Gleave et al*. AMI achieves better results than baseline under different λ .

Finally, we check the performance of AMI under different hyperparameters λ , which controls the proportion of AMI reward I_t^{α} in total reward. Specifically, we tested our AMI attack on $\lambda = \{0, 0.01, 0.1, 1, 10\}$, where $\lambda = 0$ reduce to the method of *Gleave et al.* As shown in Fig. 9, using AMI improves the overall performance of attack comparing with *Gleave et al.* demonstrating the effectiveness of our method, while using proper hyperparameter leads to the best performance of AMI

 $(\lambda = 0.1 \text{ in } 3s5z \text{ vs } 3s6z \text{ and } \lambda = 1 \text{ in } HalfCheetah 6x1)$. We also find the performance does not improve monotonically with arbitrarily large λ , this could be explained by (1) large λ yields high reward, which brings instability when training critic network. (2) By having large λ , errors in opponent modelling module p_{ϕ} accumulate, leading to an overly large emphasis on attack capability of next timestep.

5.5 Discussions

5.5.1 Comparing with mutual information

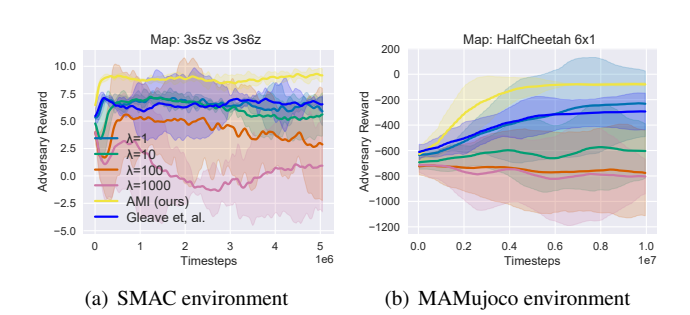


Figure 10: Using mutual information proposed in [21] as influence metric. Since mutual information is bidirectional, such metric was ineffective for attack.

We first discuss the attack capability of using mutual information as an influence metric, which can be seen as a bilateral and untargeted version of AMI. We implement mutual information by the work of [21] and test the result on four λ that control the magnitude of mutual information. As shown in Fig. 10, using mutual information oftentimes achieves worse results than *Gleave et al.* (*i.e.*, not using mutual information). Besides, the result is even worse when λ increases. This motivates us to propose AMI, a unilateral and targeted influence for c-MARL attacks, which yields superior performance.

5.5.2 Attacking other c-MARL algorithms

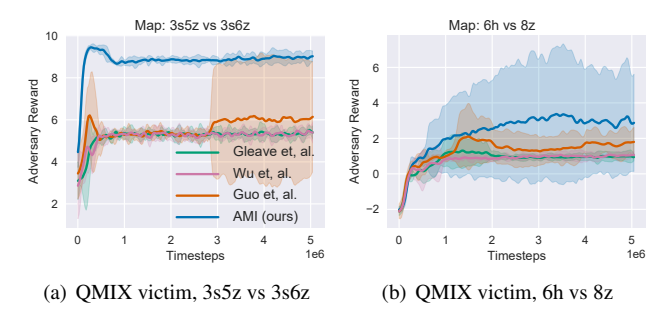


Figure 11: Attacking QMIX by AMI. The superior result of AMI is consistent in MAPPO and QMIX. MAMujoco is not evaluated since QMIX does not support continuous control.

Previously, we have shown AMI achieves superior result in attacking MAPPO victims, a representative actor-critic based

method in c-MARL. We show AMI is equally applicable to Q-learning based methods, such as QMIX [42]. As shown in Fig. 11, our AMI continues to achieve superior results comparing with baseline adversarial policy methods in 3s5z vs 3s6z and 6h vs 8z environments. We conduct experiments on SMAC environment only since Q-learning based methods do not support continuous control.

5.5.3 Aiding state-based c-MARL adversary with AMI

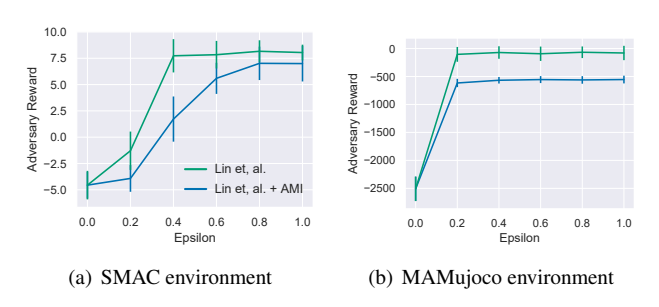


Figure 12: Using AMI as adversarial policy for state-based c-MARL adversary. AMI improves the power of state-based adversary by learning a more harmful policy under multiple perturbation budgets ε . $\varepsilon = 0$ refers to no attack.

While AMI achieves superior results comparing with baseline policy-based attack, since observation-based attack in c-MARL [30] aids their attack with adversarial policy, we can also improve the performance of their attacks by using our AMI as a more powerful adversarial policy. Following the method described by Lin et al. [30], we replace the stage 1 attack of Lin et al. from the c-MARL extension of Gleave et al. to our AMI attack, while keeping the stage 2 attack unchanged (i.e., we generate observation perturbation using the same gradient-based method). The ℓ_{∞} perturbation budget ε on observation is set to $\{0,0.2,0.4,0.6,0.8,1\}$. Note that $\varepsilon = 0$ refers to no attack. The result is shown in Fig. 12. Since observation-based attack also relies on adversarial policy as guidance to fool victims into targeted action, AMI could be directly used to achieve better attack performance in observation-based attack, showing the generality of our proposed AMI as adversarial policy.

5.5.4 Using adversary reward for AMI

In previous adversarial policy research by *Gleave et al.* and *Wu et al.*, they assume adversary reward is the negative of victim reward, forming a *zero-sum* game between adversary and victims. The work of *Guo et al.* assumes adversary holds its own objective, thus forming a *general-sum* setting and achieves stronger attack capability by jointly minimizing victim reward and maximizing adversary reward. However, in practice, it can be hard for adversary to acquire victim rewards in general-sum games due to black-box assumption. Thus, our AMI keeps the general-sum setting, but assumes

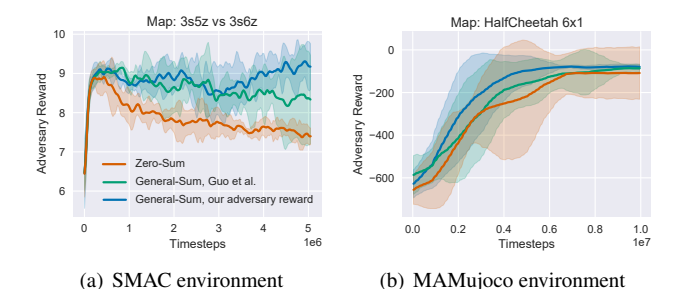


Figure 13: Attack capability of using reward setting of zerosum, general-sum proposed by *Guo et al.* and our general-sum adversarial reward. Our general-sum reward achieves the best attack capability.

access to adversary reward only, which can be freely defined and calculated from observation. We empirically evaluate the attack capability of using these three types of rewards. As illustrated in Fig. 13, modelling adversarial attack as a general-sum game achieves higher attack capability (SMAC) and better convergence in training (MAMujoco) than zero-sum setting. Moreover, in general-sum games, our adversary reward achieves better results comparing with the objective used by *Guo et al.*, showing that minimizing victim reward is not a prerequisite for general-sum attack to be strong. Consequently, since our general-sum adversarial reward brings overall better attack capability, for fair comparison, we use this reward to train our AMI attack and all baselines.

5.6 Analyzation of AMI policies

To analyze the attack strategy of AMI, we visualize victim behaviors under AMI attack on 10m vs 11m environment in Fig. 14 and 15. We find several key observations as follows:

Victim behavior under AMI. Victims attacked by AMI show two key behaviors that lead to its failure: (1) *delayed arrival*. As shown in Fig. 14, victims were influenced by the attacker and separated into two groups. The two groups encounter enemies in different timesteps: while a part of victims is facing the full strength of enemies, the other part is still approaching enemies and do not have enemies in its fire range. (2) *unfocused fire*. In SMAC, focus fire means allies jointly attack and kill enemies one after another. However, with the presence of the attacker, allies fire in an *unfocused* way. As shown in Fig. 15(d), victim fires on enemies (action id 5-15) are randomly dispersed, rather than having a cooperative target. As a result, victims failed to take down enemy units, thus facing stronger fire from enemies.

Influence through the lens of TAO. Victim behavior under AMI can be explained by the target action generated by TAO. As shown in Fig. 15, to understand *delayed arrival*, at the beginning of the game, victims 3 and 7 were encouraged to move north (action id 1), thus will arrive late comparing with agents that go east directly; As an agent going east, vic-

tim 9 was encouraged to move west or stay idle: had it follow this target, it will arrive slightly later than agents moving east directly (*i.e.*, not being influenced), but still earlier than agents moving north, which also forms delayed arrival. To understand *unfocused fire*, agents 3, 7 and 9 were encouraged to attack *different* enemies at current timestep. In this way, each enemy was attacked by a limited number of victims, thus suppressing focused fire.

Adaptive target generation. Additionally, we find TAO can generate adaptive policies for victims with different susceptibility, as shown in Fig. 15. By calculating AMI, we find agents 3 and 9 were influenced more, while their target policy learned by TAO is more deterministic. In this way, TAO generates a *targeted* goal for susceptible agents since they have a higher probability of being influenced towards the jointly worst target policy. On the other hand, as agent 7 is less influenced, the target policy learned by TAO is less deterministic. In this way, TAO generates an *untargeted* goal for insusceptible agents: as their policy can hardly be influenced, the attacker gains best results by affecting them not to play the optimal policy at the current timestep. In this way, TAO automatically learns different policies for susceptible and insusceptible victims under current attacks.

6 Countermeasures Against AMI

In this section, we propose two possible defenses and evaluate our AMI against them, including adversarial training and adversarial detection. Specifically, adversarial training re-train victim agents to maximize the performance with and without the presence of adversary, while adversarial detection trains a binary classifier to detect if adversary exists at each timestep. Again, we select 3s5z vs 3s6z for SMAC environment and HalfCheetah6x1 for MAMujoco environment as our testbed.

6.1 Adversarial Training

Adversarial training (AT) is a general approach to improve the robustness of reinforcement learning, which trains victim policy to maximize reward under the presence of adversary. We adopt the *dual training* approach used by [12, 15] to c-MARL setting, such that at each episode (*i.e.*, one round of game), victims are trained to play with the 1st agent, either as AMI adversary with fixed policy network parameters, or the benign policy executed by current victims. In this way, victims can perform well with and without attack, instead of being able to defend adversary but fail when no attack exists.

Albeit adversarial training offers promising defense against the fixed AMI adversary, we further evaluate if such defense can be broken by new adversaries. We propose two countermeasures against adversarial trained victims: (1) *re-AMI*. It is unclear if adversarial trained victims can be re-attacked by a newly trained adversary. Following [12], we re-train a new AMI adversary at the same position (*i.e.*, 1st agent) against



Figure 14: Understanding the behavior of AMI. Attacker and victims in red, enemies in blue. (a) attackers entice victims to get back. (b) victims were influenced into a bad position. (c) some victims encounter enemies, while others are still moving. (d) first-arrived victims died, and enemies focused fire on the rest. (e) attacker moves near to get killed.

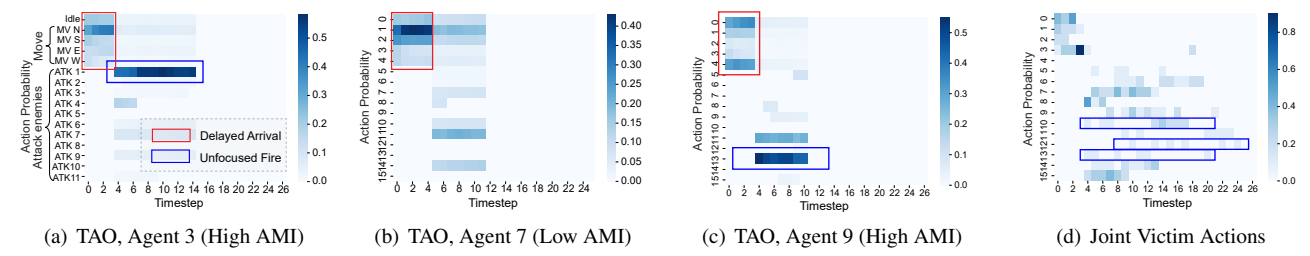


Figure 15: Illustration for actions suggested by TAO and taken by victims, evaluated in 10m vs 11m. Red and blue bracket indicates delayed arrival and unfocused fire behavior of AMI. MV N means move north and ATK X means attack enemy ID X.

adversarial trained victims. (2) *pos-AMI*. While adversarial trained victims are robust against adversary agent in certain position (e.g., 1^{st} agent as adversary), it is unsure if such victims are robust against adversary in another position (e.g., 2^{nd} agent). This threat is unique to c-MARL.

Table 2: Adversarial training (AT) results on SMAC and MA-Mujoco, adversarial reward reported with mean and standard deviation (lower means higher robustness).

Adversary	Victims	3s5z vs 3s6z	HalfCheetah 6x1
None	Normal	$-4.399_{\pm 3.917}$	$-2310.18_{\pm 666.81}$
None	AT	$-4.928_{\pm 3.779}$	$-2040.29_{\pm 75.22}$
AMI	Normal	$9.008_{\pm 2.900}$	$-72.57_{\pm 54.81}$
Alvii	AT	5.843 _{±4.612}	$-1456.62_{\pm 48.18}$
Re-AMI	Normal	$7.996_{\pm 4.015}$	$-620.14_{\pm 20.04}$
KC-AWII	AT	5.111 _{±5.365}	$-18.40_{\pm 16.76}$
Pos-AMI	Normal	$10.366_{\pm 1.774}$	$-352.11_{\pm 84.61}$
1 05-AWII	AT	8.231 _{±3.624}	$-1237.92_{\pm 68.82}$

For better comparison, we summarize the results of two types of victims (*i.e.*, normally trained victims and adversarially trained victims) against four types of adversary (*i.e.*, no adversaries, AMI, re-AMI, and Pos-AMI) in Table. 2. We can draw several conclusions as follows:

- (1) As a general defense approach, adversarial training can defend our AMI attack if defender knows the policy and position of adversary (-3.16 adversarial reward for 3s5z vs 3s6z and -1384.05 for HalfCheetah 6x1). Additionally, such defense does not largely decay normal performance without attack (-0.529 for 3s5z vs 3s6z and +269.89 for HalfCheetah 6x1). We even witness adversarial training slightly improves normal performance in 3s5z vs 3s6z.
 - (2) While adversarially trained victims are robust to re-

AMI in 3s5z vs 3s6z, it is not robust in HalfCheetah 6x1, showing the possibility of adversarial trained agents to be re-attacked. We hypothesize the non-robustness originates from the number of weaknesses in c-MARL policies: in 3s5z vs 3s6z, victim policies might have a very limited number of vulnerabilities. Through adversarial training, all weaknesses are fixed and re-training AMI cannot find more weaknesses. However, in HalfCheetah 6x1, victim policies might have many intrinsic weaknesses. While adversarial training may not fix all weaknesses, re-training AMI can still attack the policy through other vulnerabilities. For vulnerability against re-AMI, we hypothesize that it is possible to further improve robustness by iterating the process of adversarial training using re-trained AMI policy and training new AMI policy against the new victims.

(3) Additionally, we find adversarial training improves robustness over pos-AMI to some extent (-2.135 in 3s5z vs 3s6z and -885.81 in HalfCheetah 6x1), but are still less robust comparing with the AMI policy that were adversarial trained against (+2.39 in 3s5z vs 3s6z and +218.7 in HalfCheetah 6x1). The result can be interpreted as follows: first, some weakness in victim policies are position-agnostic. For example, AMI in different positions can affect victims to take similar inferior actions. Eliminating such position-agnostic weakness generalize the defense capability of adversarial training towards the 1st adversary to other positions; second, since pos-AMI adversary are equipped with different initialization and functionality, it can maximize its attack capability by probing *position-specific* vulnerabilities in victim policies. Thus, building robust c-MARL policy towards policy-based attack must take both position-agnostic and position-specific vulnerabilities in concern.

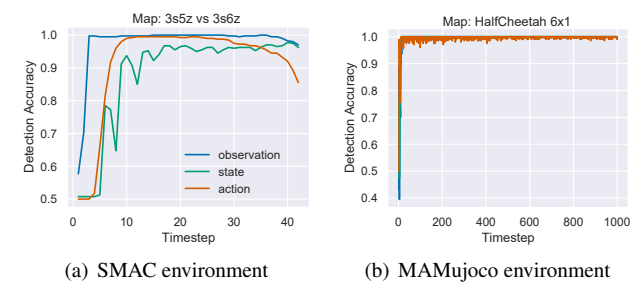


Figure 16: Adversarial detection. The presence of our AMI adversarial agent can be detected easily via using a classifier trained by observation, state or action. Adversary gets easier to detect as time proceeds.

6.2 Adversarial Detection

Adversarial detection is a prevailing approach for adversarial robustness. Instead of training victim policies such that victims can perform well under the presence of adversaries, adversarial detection detects the presence of adversary only. Specifically, we train a LSTM encoder [16] using (1) joint local observations (2) joint actions (3) global state of a full episode, and use the representation given at each timestep for binary prediction (i.e., attack/no attack). For generality, we collect a database consisting 100 game episodes without attack and 100 game episodes with attacks using the method of Gleaves et al., train our classifier on this database, and test if the classifier can detect possible AMI attack at each timestep. In this way, we can evaluate if the detection can be generalized to unseen attacks, instead of overfitting to attackspecific patterns. From results shown in Table. 16, we can draw several conclusions as follows:

- (1) AMI can be detected at high accuracy (\geq 95%) using observation, state or action. Moreover, this detection accuracy can be achieved starting at the 3^{rd} timestep for SMAC and the 12^{th} timestep for MAMujoco, showing possibility to recognize this attack at early stage. However, defending our attack can still be difficult and might require human assistance.
- (2) The accuracy of adversarial detection increases over time. Since adversary takes sequential adversarial actions to affect the victim, our classifier gets more evidence to classify if current status contains an adversary. One notable exemption is using joint actions as input in SMAC environment. In StarCraft game, most agents died when the battle is about to end. Those dead agents take a specific action to indicate their death, creating similar input which confuse the classifier.

7 Conclusion and Future Work

This paper propose AMI as the first practical black-box adversarial policy attack to evaluate the robustness of c-MARL, such that attacker unilaterally influences victims to form a worst-case cooperation. First, we adapt the agent-wise bilateral mutual information to a unilateral adversary-victim

influence for policy-based attack. This is achieved by decomposing mutual information and filtering out influence from victims to adversary. Second, to maximize team reward, we learn an reinforcement learning agent to generate the jointly worst-case target for attacker to influence. The effectiveness of our attack was verified by extensive experiments on 12 tasks on continuous and discrete control, as well as one robotic swarm control environment in real world.

While achieving promising attack capability, there still exists several directions that we hope to explore. First, while AMI does not require assess to victim parameters and observations, it still requires million iterations interacting with victim agents for successful attack, which might be impossible in real world. We would like to improve the transferability and generalization capability of our AMI attack, such that hackers can train AMI in a simulated environment with surrogate victim policy, and still achieve high attack capability by directly deploying this policy to real world. Second, we find adversarial training techniques cannot defend our AMI attack reliably. We will address the unique robustness challenge and propose defense algorithms against our AMI attack in the near future. Finally, as a first-step exploration on c-MARL agents, we hope to extend our AMI attack to mixed cooperative-competitive game in the future.

8 Ethics Statement

Cooperative multi-agent reinforcement learning (c-MARL) has been widely used in many applications, e.g., traffic light control [62], distributed resource allocation [70], cooperative swarm control [20, 40, 69], etc. However, little work has been conducted to evaluate its robustness under adversarial attack. By mimicking adversaries, strong and practical adversarial attack serves as a reliable testing algorithm towards c-MARL. Comparing with previous weak and impractical observation-based adversarial attacks for c-MARL, our paper proposes adversarial minority influence (AMI), which evaluates c-MARL robustness under a practical black-box setting, with strong attack capability. Experiments on continuous, discrete control, as well as simulation and real world environment reveals the ubiquitous vulnerability of c-MARL agents against adversarial policy, drawing research attention to this novel yet important security scenario. To mitigate AMI attack, we propose two countermeasures, and find while discovering AMI attack can be easy, due to the unique complexity of c-MARL, the attack cannot be trivially defended, calling an urgent need for defense on c-MARL policies. All experiments are conducted on public-available, open-source simulation environments and laboratory robotic environments, with no human subjects or sensitive data involved.

References

- [1] Vahid Behzadan and William Hsu. Sequential triggers for watermarking of deep reinforcement learning policies. *arXiv preprint arXiv:1906.01126*, 2019.
- [2] Sushrut Bhalla, Sriram Ganapathi Subramanian, and Mark Crowley. Deep multi agent reinforcement learning for autonomous driving. In *Canadian Conference on Artificial Intelligence*, pages 67–78. Springer, 2020.
- [3] Jan Blumenkamp and Amanda Prorok. The emergence of adversarial communication in multi-agent reinforcement learning. In *Conference on Robot Learning*, pages 1394–1414. PMLR, 2021.
- [4] Nicholas Carlini and David Wagner. Towards evaluating the robustness of neural networks. In 2017 ieee symposium on security and privacy (sp), pages 39–57. IEEE, 2017.
- [5] William D Crano and Viviane Seyranian. Majority and minority influence. *Social and Personality Psychology Compass*, 1(1):572–589, 2007.
- [6] Nikolay Dandanov, Hussein Al-Shatri, Anja Klein, and Vladimir Poulkov. Dynamic self-optimization of the antenna tilt for best trade-off between coverage and capacity in mobile networks. Wireless Personal Communications, 92(1):251–278, 2017.
- [7] Christian Schroeder de Witt, Tarun Gupta, Denys Makoviichuk, Viktor Makoviychuk, Philip HS Torr, Mingfei Sun, and Shimon Whiteson. Is independent learning all you need in the starcraft multi-agent challenge? arXiv preprint arXiv:2011.09533, 2020.
- [8] Ammar Fayad and Majd Ibrahim. Influence-based reinforcement learning for intrinsically-motivated agents. *arXiv preprint arXiv:2108.12581*, 2021.
- [9] Jakob Foerster, Gregory Farquhar, Triantafyllos Afouras, Nantas Nardelli, and Shimon Whiteson. Counterfactual multi-agent policy gradients. In *Proceedings of the AAAI conference on artificial intelligence*, volume 32, 2018.
- [10] Antonis Gardikiotis. Minority influence. *Social and personality psychology compass*, 5(9):679–693, 2011.
- [11] Sait Murat Giray. Anatomy of unmanned aerial vehicle hijacking with signal spoofing. In 2013 6th International Conference on Recent Advances in Space Technologies (RAST), pages 795–800. IEEE, 2013.
- [12] Adam Gleave, Michael Dennis, Cody Wild, Neel Kant, Sergey Levine, and Stuart Russell. Adversarial policies: Attacking deep reinforcement learning. *arXiv preprint arXiv:1905.10615*, 2019.

- [13] Ian J Goodfellow, Jonathon Shlens, and Christian Szegedy. Explaining and harnessing adversarial examples. *arXiv* preprint arXiv:1412.6572, 2014.
- [14] Jun Guo, Yonghong Chen, Yihang Hao, Zixin Yin, Yin Yu, and Simin Li. Towards comprehensive testing on the robustness of cooperative multi-agent reinforcement learning. In *Proceedings of the IEEE/CVF Conference* on Computer Vision and Pattern Recognition, pages 115– 122, 2022.
- [15] Wenbo Guo, Xian Wu, Sui Huang, and Xinyu Xing. Adversarial policy learning in two-player competitive games. In *International Conference on Machine Learn*ing, pages 3910–3919. PMLR, 2021.
- [16] Sepp Hochreiter and Jürgen Schmidhuber. Long short-term memory. *Neural computation*, 9(8):1735–1780, 1997.
- [17] Sebastian Höfer, Kostas Bekris, Ankur Handa, Juan Camilo Gamboa, Melissa Mozifian, Florian Golemo, Chris Atkeson, Dieter Fox, Ken Goldberg, John Leonard, et al. Sim2real in robotics and automation: Applications and challenges. *IEEE transactions* on automation science and engineering, 18(2):398–400, 2021.
- [18] Sandy Huang, Nicolas Papernot, Ian Goodfellow, Yan Duan, and Pieter Abbeel. Adversarial attacks on neural network policies. *arXiv preprint arXiv:1702.02284*, 2017.
- [19] Yunhan Huang and Quanyan Zhu. Deceptive reinforcement learning under adversarial manipulations on cost signals. In *International Conference on Decision and Game Theory for Security*, pages 217–237. Springer, 2019.
- [20] Maximilian Hüttenrauch, Sosic Adrian, Gerhard Neumann, et al. Deep reinforcement learning for swarm systems. *Journal of Machine Learning Research*, 20(54):1–31, 2019.
- [21] Natasha Jaques, Angeliki Lazaridou, Edward Hughes, Caglar Gulcehre, Pedro Ortega, DJ Strouse, Joel Z Leibo, and Nando De Freitas. Social influence as intrinsic motivation for multi-agent deep reinforcement learning. In *International conference on machine learning*, pages 3040–3049. PMLR, 2019.
- [22] Ahmad Ali Khan and Raviraj S Adve. Centralized and distributed deep reinforcement learning methods for downlink sum-rate optimization. *IEEE Transactions on Wireless Communications*, 19(12):8410–8426, 2020.

- [23] Ahmed Yar Khan, Rabia Latif, Seemab Latif, Shahzaib Tahir, Gohar Batool, and Tanzila Saba. Malicious insider attack detection in iots using data analytics. *IEEE Access*, 8:11743–11753, 2019.
- [24] Woojun Kim, Whiyoung Jung, Myungsik Cho, and Youngchul Sung. A maximum mutual information framework for multi-agent reinforcement learning. arXiv preprint arXiv:2006.02732, 2020.
- [25] Panagiota Kiourti, Kacper Wardega, Susmit Jha, and Wenchao Li. Trojdrl: Trojan attacks on deep reinforcement learning agents. arXiv preprint arXiv:1903.06638, 2019.
- [26] Jernej Kos and Dawn Song. Delving into adversarial attacks on deep policies. *arXiv preprint* arXiv:1705.06452, 2017.
- [27] Jakub Grudzien Kuba, Ruiqing Chen, Munning Wen, Ying Wen, Fanglei Sun, Jun Wang, and Yaodong Yang. Trust region policy optimisation in multi-agent reinforcement learning. arXiv preprint arXiv:2109.11251, 2021.
- [28] Kaya Kuru, Darren Ansell, Wasiq Khan, and Halil Yetgin. Analysis and optimization of unmanned aerial vehicle swarms in logistics: An intelligent delivery platform. *Ieee Access*, 7:15804–15831, 2019.
- [29] Pengyi Li, Hongyao Tang, Tianpei Yang, Xiaotian Hao, Tong Sang, Yan Zheng, Jianye Hao, Matthew E Taylor, and Zhen Wang. Pmic: Improving multi-agent reinforcement learning with progressive mutual information collaboration. arXiv preprint arXiv:2203.08553, 2022.
- [30] Jieyu Lin, Kristina Dzeparoska, Sai Qian Zhang, Alberto Leon-Garcia, and Nicolas Papernot. On the robustness of cooperative multi-agent reinforcement learning. In 2020 IEEE Security and Privacy Workshops (SPW), pages 62–68. IEEE, 2020.
- [31] Yen-Chen Lin, Zhang-Wei Hong, Yuan-Hong Liao, Meng-Li Shih, Ming-Yu Liu, and Min Sun. Tactics of adversarial attack on deep reinforcement learning agents. *arXiv preprint arXiv:1703.06748*, 2017.
- [32] Michael L Littman. Markov games as a framework for multi-agent reinforcement learning. In *Machine learning proceedings 1994*, pages 157–163. Elsevier, 1994.
- [33] Ryan Lowe, Yi I Wu, Aviv Tamar, Jean Harb, OpenAI Pieter Abbeel, and Igor Mordatch. Multi-agent actor-critic for mixed cooperative-competitive environments. *Advances in neural information processing systems*, 30, 2017.

- [34] Bora Ly and Romny Ly. Cybersecurity in unmanned aerial vehicles (uavs). *Journal of Cyber Security Technology*, 5(2):120–137, 2021.
- [35] Rupert Mitchell, Jan Blumenkamp, and Amanda Prorok. Gaussian process based message filtering for robust multi-agent cooperation in the presence of adversarial communication. *arXiv* preprint arXiv:2012.00508, 2020.
- [36] Francesco Mondada, Michael Bonani, Xavier Raemy, James Pugh, Christopher Cianci, Adam Klaptocz, Stephane Magnenat, Jean-Christophe Zufferey, Dario Floreano, and Alcherio Martinoli. The e-puck, a robot designed for education in engineering. In *Proceedings of the 9th conference on autonomous robot systems and competitions*, volume 1, pages 59–65. IPCB: Instituto Politécnico de Castelo Branco, 2009.
- [37] Praveen Palanisamy. Multi-agent connected autonomous driving using deep reinforcement learning. In 2020 International Joint Conference on Neural Networks (IJCNN), pages 1–7. IEEE, 2020.
- [38] Nicolas Papernot, Patrick McDaniel, Somesh Jha, Matt Fredrikson, Z Berkay Celik, and Ananthram Swami. The limitations of deep learning in adversarial settings. In 2016 IEEE European symposium on security and privacy (EuroS&P), pages 372–387. IEEE, 2016.
- [39] Georgios Papoudakis, Filippos Christianos, Lukas Schäfer, and Stefano V Albrecht. Benchmarking multiagent deep reinforcement learning algorithms in cooperative tasks. arXiv preprint arXiv:2006.07869, 2020.
- [40] Bei Peng, Tabish Rashid, Christian Schroeder de Witt, Pierre-Alexandre Kamienny, Philip Torr, Wendelin Böhmer, and Shimon Whiteson. Facmac: Factored multiagent centralised policy gradients. Advances in Neural Information Processing Systems, 34:12208–12221, 2021
- [41] Amin Rakhsha, Goran Radanovic, Rati Devidze, Xiaojin Zhu, and Adish Singla. Policy teaching via environment poisoning: Training-time adversarial attacks against reinforcement learning. In *International Conference on Machine Learning*, pages 7974–7984. PMLR, 2020.
- [42] Tabish Rashid, Mikayel Samvelyan, Christian Schroeder, Gregory Farquhar, Jakob Foerster, and Shimon Whiteson. Qmix: Monotonic value function factorisation for deep multi-agent reinforcement learning. In *Interna*tional conference on machine learning, pages 4295– 4304. PMLR, 2018.
- [43] Nils Miro Rodday, Ricardo de O Schmidt, and Aiko Pras. Exploring security vulnerabilities of unmanned aerial

- vehicles. In NOMS 2016-2016 IEEE/IFIP Network Operations and Management Symposium, pages 993–994. IEEE, 2016.
- [44] Amiya Kumar Sahu, Suraj Sharma, and Deepak Puthal. Lightweight multi-party authentication and key agreement protocol in iot-based e-healthcare service. *ACM Transactions on Multimedia Computing, Communications, and Applications (TOMM)*, 17(2s):1–20, 2021.
- [45] Farhan A Salem. Dynamic and kinematic models and control for differential drive mobile robots. *International Journal of Current Engineering and Technology*, 3(2):253–263, 2013.
- [46] Mikayel Samvelyan, Tabish Rashid, Christian Schroeder De Witt, Gregory Farquhar, Nantas Nardelli, Tim GJ Rudner, Chia-Man Hung, Philip HS Torr, Jakob Foerster, and Shimon Whiteson. The starcraft multi-agent challenge. arXiv preprint arXiv:1902.04043, 2019.
- [47] John Schulman, Philipp Moritz, Sergey Levine, Michael Jordan, and Pieter Abbeel. High-dimensional continuous control using generalized advantage estimation. *arXiv* preprint arXiv:1506.02438, 2015.
- [48] John Schulman, Filip Wolski, Prafulla Dhariwal, Alec Radford, and Oleg Klimov. Proximal policy optimization algorithms. *arXiv preprint arXiv:1707.06347*, 2017.
- [49] Shai Shalev-Shwartz, Shaked Shammah, and Amnon Shashua. Safe, multi-agent, reinforcement learning for autonomous driving. *arXiv preprint arXiv:1610.03295*, 2016.
- [50] Kyunghwan Son, Daewoo Kim, Wan Ju Kang, David Earl Hostallero, and Yung Yi. Qtran: Learning to factorize with transformation for cooperative multiagent reinforcement learning. In *International conference on machine learning*, pages 5887–5896. PMLR, 2019.
- [51] Yanchao Sun, Ruijie Zheng, Yongyuan Liang, and Furong Huang. Who is the strongest enemy? towards optimal and efficient evasion attacks in deep rl. *arXiv* preprint arXiv:2106.05087, 2021.
- [52] Peter Sunehag, Guy Lever, Audrunas Gruslys, Wojciech Marian Czarnecki, Vinicius Zambaldi, Max Jaderberg, Marc Lanctot, Nicolas Sonnerat, Joel Z Leibo, Karl Tuyls, et al. Value-decomposition networks for cooperative multi-agent learning. arXiv preprint arXiv:1706.05296, 2017.
- [53] Christian Szegedy, Wojciech Zaremba, Ilya Sutskever, Joan Bruna, Dumitru Erhan, Ian Goodfellow, and Rob Fergus. Intriguing properties of neural networks. *arXiv* preprint arXiv:1312.6199, 2013.

- [54] Ardi Tampuu, Tambet Matiisen, Dorian Kodelja, Ilya Kuzovkin, Kristjan Korjus, Juhan Aru, Jaan Aru, and Raul Vicente. Multiagent cooperation and competition with deep reinforcement learning. *PloS one*, 12(4):e0172395, 2017.
- [55] Emanuel Todorov, Tom Erez, and Yuval Tassa. Mujoco: A physics engine for model-based control. In 2012 IEEE/RSJ international conference on intelligent robots and systems, pages 5026–5033. IEEE, 2012.
- [56] James Tu, Tsunhsuan Wang, Jingkang Wang, Sivabalan Manivasagam, Mengye Ren, and Raquel Urtasun. Adversarial attacks on multi-agent communication. In *Pro*ceedings of the IEEE/CVF International Conference on Computer Vision, pages 7768–7777, 2021.
- [57] Jianhao Wang, Zhizhou Ren, Terry Liu, Yang Yu, and Chongjie Zhang. Qplex: Duplex dueling multi-agent q-learning. *arXiv preprint arXiv:2008.01062*, 2020.
- [58] Lun Wang, Zaynah Javed, Xian Wu, Wenbo Guo, Xinyu Xing, and Dawn Song. Backdoorl: Backdoor attack against competitive reinforcement learning. *arXiv* preprint arXiv:2105.00579, 2021.
- [59] Tonghan Wang, Jianhao Wang, Yi Wu, and Chongjie Zhang. Influence-based multi-agent exploration. *arXiv* preprint arXiv:1910.05512, 2019.
- [60] Fan Wu, Linyi Li, Chejian Xu, Huan Zhang, Bhavya Kailkhura, Krishnaram Kenthapadi, Ding Zhao, and Bo Li. Copa: Certifying robust policies for offline reinforcement learning against poisoning attacks. arXiv preprint arXiv:2203.08398, 2022.
- [61] Jun Wu and Xin Xu. Decentralised grid scheduling approach based on multi-agent reinforcement learning and gossip mechanism. *CAAI Transactions on Intelligence Technology*, 3(1):8–17, 2018.
- [62] Tong Wu, Pan Zhou, Kai Liu, Yali Yuan, Xiumin Wang, Huawei Huang, and Dapeng Oliver Wu. Multi-agent deep reinforcement learning for urban traffic light control in vehicular networks. *IEEE Transactions on Vehicular Technology*, 69(8):8243–8256, 2020.
- [63] Xian Wu, Wenbo Guo, Hua Wei, and Xinyu Xing. Adversarial policy training against deep reinforcement learning. In 30th USENIX Security Symposium (USENIX Security 21), pages 1883–1900, 2021.
- [64] Wanqi Xue, Wei Qiu, Bo An, Zinovi Rabinovich, Svetlana Obraztsova, and Chai Kiat Yeo. Mis-spoke or mis-lead: Achieving robustness in multi-agent communicative reinforcement learning. arXiv preprint arXiv:2108.03803, 2021.

- [65] Yaodong Yang and Jun Wang. An overview of multiagent reinforcement learning from game theoretical perspective. *arXiv* preprint arXiv:2011.00583, 2020.
- [66] Zhaoyuan Yang, Naresh Iyer, Johan Reimann, and Nurali Virani. Design of intentional backdoors in sequential models. *arXiv preprint arXiv:1902.09972*, 2019.
- [67] Dayon Ye, Minji Zhang, and Yu Yang. A multi-agent framework for packet routing in wireless sensor networks. *sensors*, 15(5):10026–10047, 2015.
- [68] Chao Yu, Akash Velu, Eugene Vinitsky, Yu Wang, Alexandre Bayen, and Yi Wu. The surprising effectiveness of ppo in cooperative, multi-agent games. *arXiv* preprint arXiv:2103.01955, 2021.
- [69] Won Joon Yun, Soohyun Park, Joongheon Kim, Myung-Jae Shin, Soyi Jung, David A Mohaisen, and Jae-Hyun Kim. Cooperative multiagent deep reinforcement learning for reliable surveillance via autonomous multi-uav control. *IEEE Transactions on Industrial Informatics*, 18(10):7086–7096, 2022.
- [70] Chongjie Zhang, Victor Lesser, and Prashant Shenoy. A multi-agent learning approach to online distributed resource allocation. In *Twenty-first international joint conference on artificial intelligence*, 2009.
- [71] Huan Zhang, Hongge Chen, Duane Boning, and Cho-Jui Hsieh. Robust reinforcement learning on state observations with learned optimal adversary. *arXiv preprint arXiv:2101.08452*, 2021.
- [72] Huan Zhang, Hongge Chen, Chaowei Xiao, Bo Li, Mingyan Liu, Duane Boning, and Cho-Jui Hsieh. Robust deep reinforcement learning against adversarial perturbations on state observations. Advances in Neural Information Processing Systems, 33:21024–21037, 2020.
- [73] Lin Zhang and Ying-Chang Liang. Deep reinforcement learning for multi-agent power control in heterogeneous networks. *IEEE Transactions on Wireless Communications*, 20(4):2551–2564, 2020.
- [74] Ming Zhou, Jun Luo, Julian Villella, Yaodong Yang, David Rusu, Jiayu Miao, Weinan Zhang, Montgomery Alban, Iman Fadakar, Zheng Chen, et al. Smarts: Scalable multi-agent reinforcement learning training school for autonomous driving. arXiv preprint arXiv:2010.09776, 2020.

Appendix

A More Details of AMI method

A.1 More Details of Eqn. 6

We start from $-D_{KL}\left(\mathbb{E}_{\tilde{a}_{t}^{\alpha} \sim \pi_{t}^{\alpha}}\left[p_{\phi}(\hat{a}_{t+1,i}^{v}|s_{t},\tilde{a}_{t}^{\alpha},\mathbf{a}_{t}^{v})\right]||\mathcal{U})\right)$, which can be expressed as:

$$-D_{KL}\left(\mathbb{E}_{\tilde{a}_{t}^{\alpha} \sim \pi_{t}^{\alpha}}\left[p_{\phi}(\hat{a}_{t+1,i}^{\nu}|s_{t}, \tilde{a}_{t}^{\alpha}, \mathbf{a}_{t}^{\nu})\right] || \mathcal{U}\right)\right)$$

$$=-D_{KL}\left(\left[\sum_{\tilde{a}_{t}^{\alpha}}p_{\phi}(\hat{a}_{t+1,i}^{\nu}|s_{t}, \tilde{a}_{t}^{\alpha}, \mathbf{a}_{t}^{\nu}) \cdot p_{\theta}(\tilde{a}_{t}^{\alpha}|s_{t}, \mathbf{a}_{t}^{\nu})\right] || \mathcal{U}\right)\right),$$

$$=-D_{KL}\left(\left[\sum_{\tilde{a}_{t}^{\alpha}}p_{\phi}(\hat{a}_{t+1,i}^{\nu}|s_{t}, \tilde{a}_{t}^{\alpha}, \mathbf{a}_{t}^{\nu}) \cdot p_{\theta}(\tilde{a}_{t}^{\alpha}|s_{t})\right] || \mathcal{U}\right)\right),$$

$$=-D_{KL}\left(p_{\phi}(\hat{a}_{t+1,i}^{\nu}|s_{t}, \mathbf{a}_{t}^{\nu}) || \mathcal{U}\right),$$

$$=-\sum_{\hat{a}_{t+1,i} \in \mathcal{A}_{i}}p_{\phi}(\hat{a}_{t+1,i}^{\nu}|s_{t}, \mathbf{a}_{t}^{\nu}) \log\left(\frac{p_{\phi}(\hat{a}_{t+1,i}^{\nu}|s_{t}, \mathbf{a}_{t}^{\nu})}{\mathcal{U}}\right),$$

$$=-\sum_{\hat{a}_{t+1,i} \in \mathcal{A}_{i}}p_{\phi}(\hat{a}_{t+1,i}^{\nu}|s_{t}, \mathbf{a}_{t}^{\nu}) \log\left(p_{\phi}(\hat{a}_{t+1,i}^{\nu}|s_{t}, \mathbf{a}_{t}^{\nu}) - p_{\phi}(\hat{a}_{t+1,i}^{\nu}|s_{t}, \mathbf{a}_{t}^{\nu}) \log\left(\mathcal{U}\right),$$

$$=-\sum_{\hat{a}_{t+1,i} \in \mathcal{A}_{i}}p_{\phi}(\hat{a}_{t+1,i}^{\nu}|s_{t}, \mathbf{a}_{t}^{\nu}) \log\left(p_{\phi}(\hat{a}_{t+1,i}^{\nu}|s_{t}, \mathbf{a}_{t}^{\nu}) - c,$$

$$=H(\hat{a}_{t+1,i}^{\nu}|s_{t}, \mathbf{a}_{t}^{\nu}) - c.$$

$$(10)$$

Moving -c to other side completes our claim in Fig. 6, where c is a constant irrelevant to our attack. The derivation comes from standard definition of KL divergence and information theory, which indicates that maximizing minority influence is equal to minimizing the KL divergence between victim. The derivation of Eqn. 6 in continuous setting is the same as discrete setting, since the logarithm of uniform distribution \mathcal{U} is always a constant.

A.2 Majority and Minority Influence

Next, we use a toy example to motivate our claim in main paper. Under this toy example, we can calculate mutual information and optimal policy analytically. Specifically, the experiment setting is illustrated in Fig. A.1. In this experiment, we assume two agents exists, the adversary a_{adv} and a victim agent a_j with fixed policy. Both agents can only take actions to go left or right. The policy of victim agent a_j is fixed, such that it goes left at probability 0.2 and right at probability 0.8, while the policy of adversary agent a_{adv} can be adapted for attack. Its policy is conditioned on the action taken by victim, where we omit temporal dependence for simplicity, while the only parameter it can control is the probability p, such that its probability of going left or right adapts to victim action. The task of adversary a_{adv} is to change influence the action

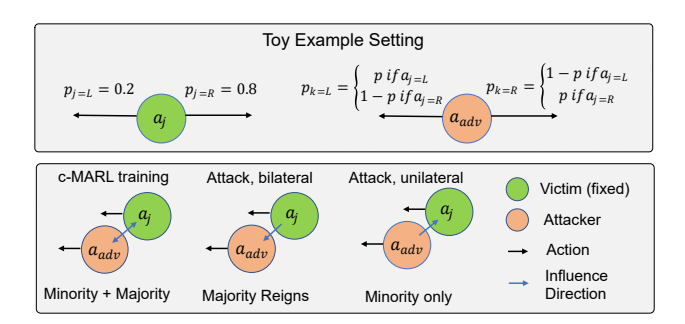


Figure A.1: Toy example used to illustrate our majority and minority influence theme. In this toy example, the adversary a_{adv} tries to influence the policy of a fixed victim agent a_j . While the a_{adv} cannot actually influence the policy of a_j , using allows a_{adv} to cheat by changing its own policy that fits to the policy of a_j .

probability of victim a_j . However, since the policy of victim agent a_j is fixed, it is actually impossible for a_{adv} to influence a_j .

As a consequence, a proper influence metric should also reflect this property, such that no matter how p changes, it is impossible to gain influence by changing p controlled by a_{adv} to affect a_j . However, in mutual information, this is not the case. As shown in Fig. 2(a), the adversary can actually affect mutual information $I(a_j;a_{adv})$ by changing its own action probability p. While the probability of $p(a_j)$ is fixed, calculating mutual information relies on the joint action probability $p(a_j,a_{adv})$, leaving space for adversary to change its action probability that influence mutual information. Specifically, to be maximally informative of a_j , a_{adv} can change its policy to be maximally predictive of a_j . Thus, adversary maximize its mutual information between itself and victim by overfitting to the policy of victim.

We shall note that this problem is unique to policy-based attack since the victim policy is fixed. As the number of agent increases, changing the action of one agent creates less impact on fixed victim parameter, such that victim will yield increasingly fixed policy (*i.e.*, action probability). However, in common c-MARL training, since all agents can adapt their policy jointly, such unexpected behavior do not exist in mutual information.

To solve this problem, note that mutual information $I(a_j; a_{adv}) = -H(a_j|a_{adv}) + H(a_j)$, where the former indicates majority influence and the latter is minority influence. As illustrated in Fig. 2(b), and Fig. 2(c), majority influence is the major source for adversary to change its own policy to overfit the adversary. However, minority influence term is free of such problem. No matter how adversary change its policy p, the magnitude of influence stays still. As a consequence, attacker cannot cheat for higher influence by changing its policy, since the reward gained remains constant.

B More Details of Simulation Environments

In this section, we introduce the environments we attack for simulation (SMAC and MAMujoco) in detail. Specifically, we introduce the environment, adversary reward, evaluation metric, and detailed attack settings.

B.1 SMAC environment

B.1.1 Introduction

StarCraftII Multi-Agent Challenge environment [46] is a widely used discrete-action environment for evaluating the effectiveness of multi-agent reinforcement learning. In SMAC, each agent can select one discrete action available at the current timestep, including moving and attacking. Specifically, we base our framework on Extended Pymarl [39], an extended version of the original code described in [46] widely used to evaluate the performance of SMAC.

B.1.2 Adversary Reward

In the original version of SMAC [46], agents were trained using a *shaped reward* of enemies, which we call it (*reward_enemies*). This reward contains three terms: (1) hitpoint damage dealt to enemies. (2) enemy units killed. (3) winning the game. However, we argue this reward cannot comprehensively evaluate the attack performance of the attacker, since the goal of the attacker is to affect its allies, while the only loss in enemies is counted. To comprehensively evaluate the attack performance of the adversary, we argue that loss in both enemies and allies should be considered. We add a symmetric version of *shaped allies reward* (*reward_allies*) that measures the exact three terms just like enemies: (1) hitpoint damage dealt to allies. (2) ally units killed. (3) losing the game. Finally, adversary reward is defined as *reward_enemies - reward_allies* and used for AMI and all other baselines.

B.1.3 Evaluation metric

After proposing our adversarial reward, we believe the winning rate is insufficient to evaluate attacker capability in SMAC environment. While original SMAC tasks seek to maximize the rate of winning, the goal of the attacker is to not only fool allies towards a failure (losing the game), but also to minimize the loss of enemies and maximize the loss of victims. It is possible that both adversary can fool victims to a winning rate of 0, but one adversary is better by additionally good at reducing the number of death of enemies. Clearly, to reduce enemy death, adversary must learn a smarter way to influence its victims to achieve this stronger result. This motivates us to use our adversarial reward to evaluate attack effort more comprehensively.

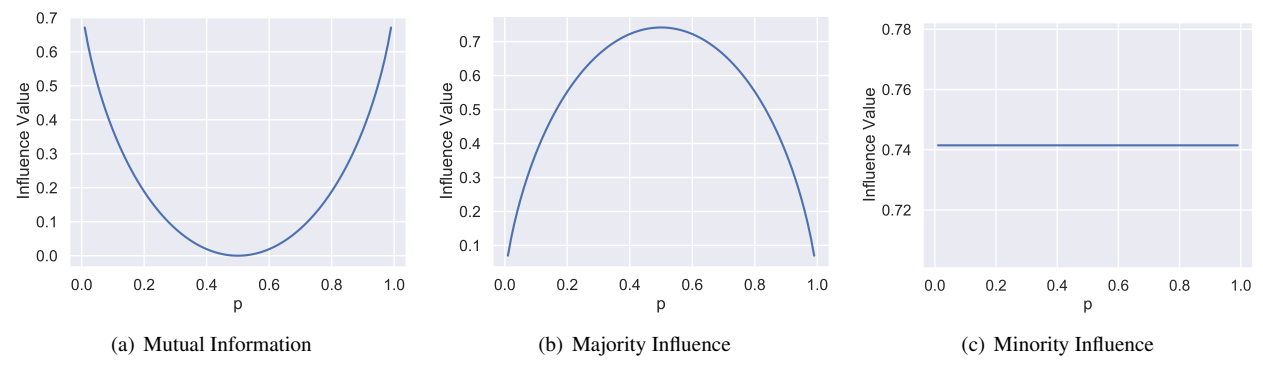


Figure A.2: The mutual information, majority influence and minority influence calculated in our toy example. In mutual information, adversary is able to maximize its influence by changing its policy p, without actually changing the action probability of a_j . This unexpected behavior originates in majority influence term in mutual information, and is not expressed in minority influence.

B.1.4 Detailed attack setting

SMAC environments differ from MAMujoco that victims combat with another group of enemies. Originally, two groups of agents have similar combat capabilities. However, the introduction of an attacker itself weakens the combat capability of victims even if we do not use adversarial policy. This leads to an unfair battle (for example, victims can never win in 10m vs 11m environment if one ally is controlled by the attacker, resulting in 9 marines controlled by MARL to combat with 11 marines controlled by heuristic AI). To fairly evaluate attacks in SMAC environment, we add an adversarial agent to the side of victims, train all victims together, then use adversarial policy to attack that added agent.

B.2 MAMujoco environment

B.2.1 Introduction

Mujoco [55] is a well-known environment where robots learn to control their joints to move in an optimal way. Multi-agent Mujoco environment [40] implements Mujoco in a multi-agent fashion, where the original robot was separated into independent parts, and the goal is to learn a strategy to move cooperatively in an optimal way. We base our framework for MAMujoco on the implementation of [27], which implements MAPPO with high performance. We use the default hyperparameters in their implementations without modification.

B.2.2 Adversary Reward

The reward of MAMujoco is similar compared with Mujoco, which contains two terms, reward_run and reward_ctrl. reward_run specifies the reward for robots achieving high forward velocity; while reward_ctrl penalizes the robot for having large a action vector magnitude. We define adversary reward as the negative of reward_run, since reward_ctrl is an auxiliary reward used in normal training and does not reflect the concern of the adversary.

C More Details of Baseline Implementations

For all baselines, we train them to maximize the adversary reward given above, adapting their method to c-MARL attack while maximally following their originally proposed methods. (1) For the method of *Guo et al.* [15], we add a central critic to estimate and minimize victim rewards, as described by their method. (2) For the method of *Wu et al.* [63], since their method is proposed for continuous control only, in continuous control, we implement their action prediction module (Eqn. 12 in their original paper) by cross-entropy loss. (3) For the observation-based attack of *Lin et al.* [30], we follow their default implementation and set the maximum attack iteration to 30. The perturbation budget is measured by ℓ_{∞} norm.

D More Details of Real-World Robot Environments

In this section, we describe the details of real-world robot environments.

D.1 Real-world environment

We perform all experiments based on a set of e-puck2 robot [36], a mini mobile robot developed by EPFL, which is a widely used robot in various research and educational scenarios. We added an expansion board with Raspberry Pi to E-puck2 robots to increase their computing power.

The experiments take place in a $2m \times 2m$ indoor arena, with walls on the boundary. We add a centralized motion capture system to capture the position of each robot, such that we can calculate the state and observation information required by [20]. To fairly compare each method and avoid the effect of initialization, in each runs (we tested all methods for 10 runs), we initialize all methods to the same position (we project the place for initialization using the blue cross projected in our arena, as shown in Fig. 4b in our main paper. Then, we man-

ually place all robots to the projected blue cross before the episode starts), while the initialization varies among different experiment runs. This corresponds to a *within-subjects* design, so we test our result using the corresponding paired samples t-test and Wilcoxon signed-rank test, respectively.

D.2 Task and reward

We conduct our simulation experiment in a rendezvous environment following the work [20]. In this environment, all robots were encouraged to meet in the same location to get the highest reward. The location can be an arbitrary valid location in the map. The reward contains two parts, $reward_distance$ (r_d) , which specifies how robots were close to each other. Similar to Mujoco [55], a penalty term $reward_control$ (r_c) was added as the L2 norm of the action each agents, in order to to penalize extremely large actions. The full reward r can be expressed as:

$$r = r_d - 0.001 \cdot r_c. \tag{11}$$

To encourage robots close to each other, *reward_distance* can be expressed as:

$$r_d = -\sum_{i=0}^{N} \sum_{j=i+1}^{N} ||\mathbf{p}_i - \mathbf{p}_j||_2,$$
 (12)

where $\mathbf{p} = (x, y)$ is the point that contains the x and y position of the current robot, N is the number of robots. Under this reward, each robot receives larger reward for being closer to each other.

As the L2 norm of actions, *reward_control* can be expressed as:

$$r_c = \sum_{i=0}^{N} ||\mathbf{a}_i||_2,\tag{13}$$

where \mathbf{a}_i is the action taken by all individual robots.

D.3 Observation and Actions

To measure and convey information of all robots, we maintain two global matrices which we use to get local and global observations: distance matrix (M_d) and angle matrix (M_a) . Each element in the distance matrix represents the Euclidean distance between two robots. As for the angle in M_a , we calculate the pairwise included angle between every two agents. As illustrated in Fig. D.1, to calculate the included angle θ of a_i comparing with a_j , the angle is calculated between the line connecting a_i and a_j and the current orientation of a_i .

The **observations** of each agents can then be calculated from M_d and M_a , which contains the distance with other agents, and 4 included angle between two agents, which can be calculated from M_a : $\cos \theta$, $\sin \theta$, $\cos \varphi$ and $\sin \varphi$. The global

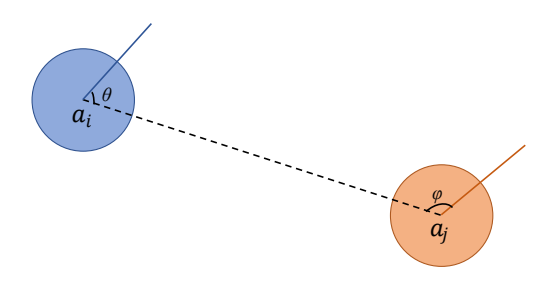


Figure D.1: The definition of angles in angle matrix M_a . Blue and orange circles a_i, a_j refer to the target robot and another robot, the solid line indicates the orientation of robots. θ is at the i-th row and j-th column of M_a , and φ is at the j-th row and i-th column of M_a .

state s^t contains the distance and angle between each individual agent:

$$s^{t} = \{M_{d}^{t}, M_{a}^{t}\}$$

$$= \{M_{d}^{t}, \theta^{t}, \phi^{t}\}.$$
(14)

The local observation o^t contains the distance and the sine and cosine value of the angle between the local agent and all other agents:

$$o_i^t = \{ M_{d,i}^t, \sin \theta_i^t, \cos \theta_i^t, \sin \varphi_i^t, \cos \varphi_i^t \}. \tag{15}$$

The **action** of the environments includes the angular velocity of two wheels of robots. The orientation of the robot is controlled by the difference of wheel velocity, driven by differential drive kinematics [45].

E Experiment Hyperparameters

In this section, we describe the hyperparameters of AMI and baselines. For **SMAC environment**, Table. E.1 describes the shared parameters used by all methods in SMAC experiments. Table. E.2 denotes the hyperparameters used for each individual methods.

Table E.1: Shared hyperparameters for SMAC, used in AMI and all baselines.

Hyperparameter	Value	Hyperparameter	Value
lr	1e-4	mini-batch num	1
parallel envs	32	max grad norm	10
gamma	0.99	max episode len	150
actor network	mlp	actor lr	=lr
hidden dim	64	critic lr	=lr
hidden layer	1	PPO epoch	4
activation	ReLU	PPO clip	0.2
optimizer	Adam	entropy coef	0.01
GAE lambda	0.95	eval episode	20

Table E.2: Method-specific parameters for Wu et al., Guo et al., and our AMI in SMAC environment.

Hyperparameters for Wu et al.					
Hyperparameter	Value	Hyperparameter	Value		
epsilon_state	0.1	epsilon_action	0.1		
lr_state	=actor lr	lr_action	=actor lr		
Hyperparameters for Guo et al.					
Hyperparameter	Value	Hyperparameter	Value		
victim critic lr	=lr				
Hyperparameters for AMI					
Hyperparameter	Value	Hyperparameter	Value		
p_{ϕ} lr	=lr	TAO lr	=lr		
TAO critic lr	=lr	AMI lambda	[.03, .05, .1]		

For **MAMujoco environment**, Table. E.3 describes the parameters used for all experiments. Table. E denotes the hyperparameters used for each individual methods.

Table E.3: Shared hyperparameters for MAMujoco, used in AMI and all baselines in MAMujoco environment.

Hyperparameter	Value	Hyperparameter	Value
parallel envs	32	mini-batch num	40
gamma	0.99	max grad norm	10
gain	0.01	max episode len	1000
actor network	mlp	actor lr	[5e-6, 5e-4]
std y coef	0.5	critic lr	5e-3
std x coef	1	Huber loss	True
hidden dim	64	Huber delta	10
hidden layer	1	PPO epoch	5
activation	ReLU	PPO clip	0.2
optimizer	Adam	entropy coef	0.01
GAE lambda	0.95	eval episode	32

For **rendezvous environment**, the hyperparameters and implementations follows MAMujoco environment, with small variations to achieve best performance in this scenario. Table. E.5 describes the parameters used for the rendezvous environment. Table. F denotes the hyperparameters used for each individual methods.

F AMI Attack in Different Positions

Besides attacking agents in different environments, due to the heterogeneity of c-MARL, agents with different IDs might have different initial positions and utility. This fact motivates us to verify if AMI is also effective when attacking agents with different initialization and functionalities. Specifically, we test AMI in 3s5z vs 3s6z environment in SMAC, with results shown in Fig. F.1. In each subfigure, adversary controls an agent with different IDs, resulting in different initialize positions and functions (as long-range Stalker or short-range Zealot). It is worth noting that in our experiment setting, we add a zealot in the left side of agents to counter the negative

Table E.4: Method-specific parameters for *Wu et al.*, *Guo et al.* and our AMI in MAMujoco environment.

Hyperparameters for Wu et al.				
Hyperparameter	Value	Hyperparameter	Value	
epsilon_state	0.1	epsilon_action	0.1	
lr_state	=actor lr	lr_action	=actor lr	
Hyperparameters for Guo et al.				
Hyperparameter	Value	Hyperparameter	Value	
victim critic lr	=lr			
Hyperparameters for AMI				
Hyperparameter	Value	Hyperparameter	Value	
p_{ϕ} lr	=lr	TAO lr	=lr	
TAO critic lr	=lr	AMI lambda	[.01, .1, .3, 1]	

Table E.5: Shared hyperparameters for rendezvous, used in AMI and all baselines.

Hy	perparameter	Value	Hyperparameter	Value
1	parallel envs	32	mini-batch num	40
	gamma	0.99	max grad norm	10
	gain	0.01	max episode len	1000
a	ctor network	mlp	actor lr	5e-5
	std y coef	0.5	critic lr	5e-3
	std x coef	1	Huber loss	True
	hidden dim	64	Huber delta	10
ŀ	nidden layer	1	PPO epoch	5
	activation	ReLU	PPO clip	0.2
	optimizer	Adam	entropy coef	0.01
(GAE lambda	0.95	eval episode	32

effect brought by the adversary, resulting in three stalkers and six zealots. Note that the attack result on agent 1 (Stalker) already illustrated in Fig. 3. Clearly, the performance of AMI is stable under different initialization and functionalities, achieving better result on 8 over 9 attack positions.

Table F.1: Method-specific parameters for *Wu et al.*, *Guo et al.*, and our AMI in rendezvous environment.

Hyperparameters for Wu et al.				
Hyperparameter	Value	Hyperparameter	Value	
epsilon_state	0.1	epsilon_action	0.1	
lr_state	=actor lr	lr_action	=actor lr	
Hyperparameters for Guo et al.				
Hyperparameter Value		Hyperparameter	Value	
victim critic lr	=lr			
Hyperparameters for AMI				
Hyperparameter	Value	Hyperparameter	Value	
p_{ϕ} lr	=lr	TAO lr	=lr	
TAO critic lr	=lr	AMI lambda	.003	

G Understanding the Variance of Guo et al.

In this section, we discuss the reason for the high variance of *Guo et al.* exhibited in MAMujoco environment, such that the high variance is not due to the use of our adversarial reward.

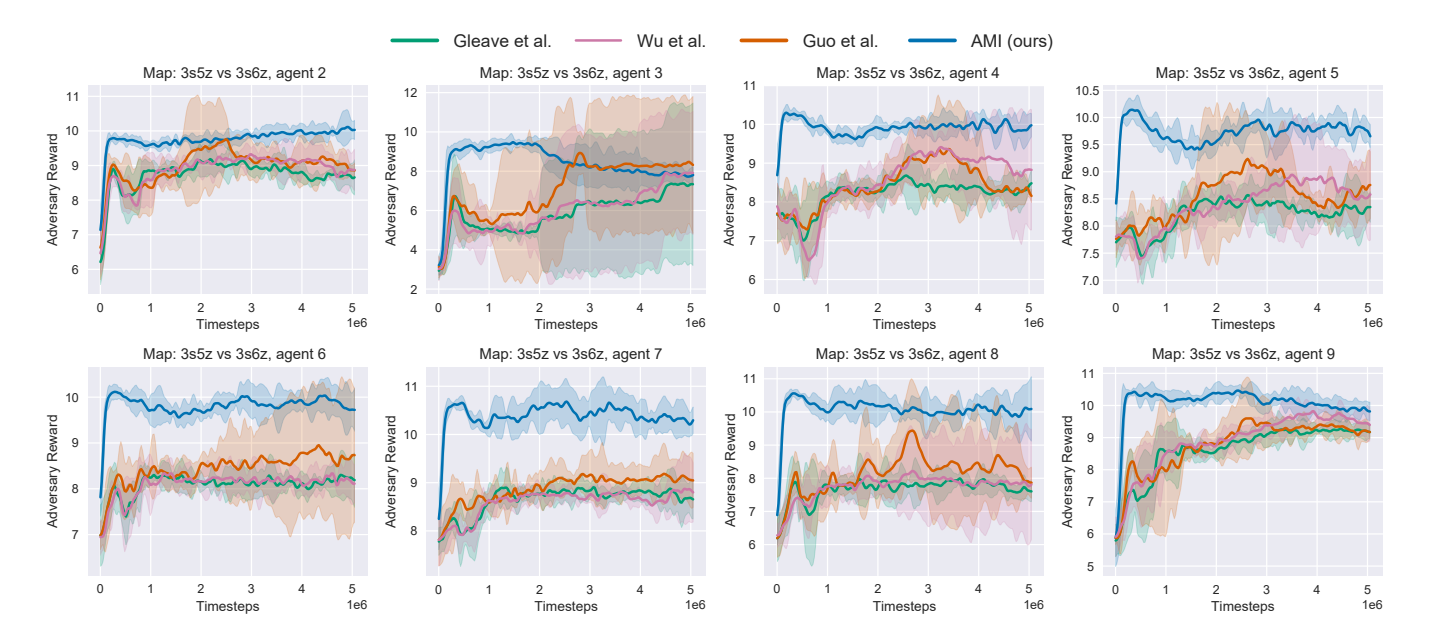


Figure F.1: Learning curves for AMI and baseline attack methods attacking agents with different IDs in 3s5z vs 3s6z environment. The agent controlled by adversary can either be a stalker or a zealot, depending on IDs of the attacker. The solid curves correspond to the mean, and the shaped region represents the 95% confidence interval over 5 random seeds.

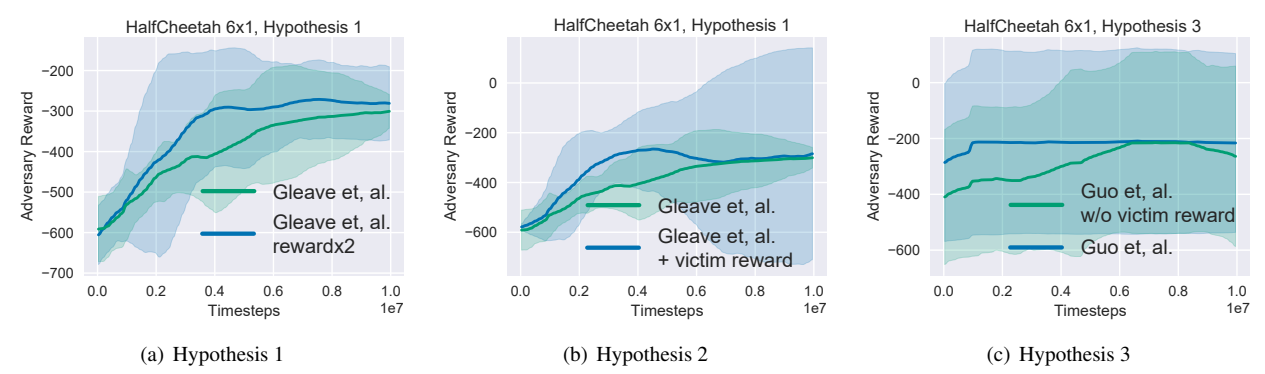


Figure F.2: Verifying the hypothesis of *Guo et al*. Our hypothesis 2 and 3 holds, which explains the high variance of *Guo et al*. is mainly due to their method and reward design.

We put forth three hypotheses:

- Hypothesis 1: the variance is due to the larger overall reward, since *Guo et al.* minimize victim reward and maximize adversary reward simultaneously. Under this reward, a learner can not converge to a good policy.
- Hypothesis 2: the variance is due to the use of victim reward, i.e., some terms in victim reward will lead to high variance.
- Hypothesis 3: the variance is due to the use of two critics, the method specifically proposed by *Guo et al*, such that the two critic structure intrinsically brings higher reward.

We verify the three hypothesis by experiments in Fig. F.2. All experiments were conducted on *HalfCheetah 6x1*.

Hypothesis 1. We design experiment to verify our first hypothesis by experimenting on *Gleave et al.*. Since the method

of *Guo et al.* is build on *Gleave et al.*, we use the method of *Gleave et al.* to disentangle the effect of reward and method. We conduct two experiments, (1) *Gleave et al.* using adversarial reward. (2) *Gleave et al.* using *doubled* adversarial reward. If larger reward impedes convergence, then *doubled* adversarial reward should exhibit higher variance. However, as shown in Fig. 2(a), higher reward magnitude does not triggers higher variance.

Hypothesis 2. We continue on the method of *Gleave et al* and test if adding victim reward to total reward creates higher variance. As shown in Fig. 2(b), our hypothesis holds, such that using victim reward will increase variance in some environments. We hypothesis this as a consequence of adding auxiliary reward terms (*i.e.*, reward_ctrl) in victim reward for victim training. These auxiliary reward can be useless in policy based attack, and thus increase variance. However, the variance after using negated victim reward is still not as large

as exhibited in *Guo et al.*, showing the high variance also stems from other roots.

Hypothesis 3. Finally, we evaluate if using different reward in the method of *Guo et al.* reduce variance. As shown in Fig. 2(b), even not using victim reward as stated in *Guo et al.*, their method still exhibits high variance. As a consequence, we hypothesis that the use of two critics that jointly updates adversary policy brings large instability, and is the main root of the variance in *Guo et al.* In contrast, our AMI use adversary reward only, and is of lower variance and better performance.

H Statistical Tests of Real-World Environment

In this section, we provide more details of statistical tests in our experiments. Our experiment uses a *within-subject design* since the initialization is fixed for all baselines in the same runs. A nonsignificant Shapiro-Wilk W test for normality on adversary reward of all methods indicates that the data are normal (for *Gleave et al.*, mean=47.59, std=4.53, W=.97, p=0.93; for *Wu et al.*, mean=47.56, std=4.21, W=.93, p=0.46; for *Guo et al.*, mean=47.81, std=5.07, W=.93, p=0.42; for AMI, mean=53.24, std=2.81, W=.95, p=0.71;).

Since the data distribution does not violate a normal distribution, we use paired samples t-test to evaluate the statistical significance between AMI and all baselines. The improvement of AMI on adversary reward is significant comparing with all methods. Specifically, AMI is significant compared with *Gleave et al.*, (t(9)=-7.08, p<.001), *Wu et al.*, (t(9)=-6.83, p<.001) and *Guo et al.*, (t(9)=-4.01, p<.05).